Atmos. Chem. Phys. Discuss., doi:10.5194/acp-2015-1039, 2016
Manuscript under review for journal Atmos. Chem. Phys.
Published: 18 January 2016
© Author(s) 2016. CC-BY 3.0 License.

Atmospheric Chemistry and Physics Discussions

Bromine atom production and chain propagation during springtime Arctic ozone depletion events in Barrow, Alaska

Chelsea R. Thompson,[1,a,b] Paul B. Shepson,[1,2] Jin Liao,[3,a,b] L. Greg Huey,[3] Chris Cantrell[4,c], Frank Flocke[4], and John Orlando[4]

[1]Department of Chemistry, Purdue University, West Lafayette, IN, USA

[2]Department of Earth and Atmospheric Sciences and Purdue Climate Change Research Center, Purdue University, West Lafayette, IN, USA

[3]School of Earth and Atmospheric Sciences, Georgia Institute of Technology, Atlanta, GA, USA

[4]National Center for Atmospheric Research, Boulder, CO, USA

[a]now at: Cooperative Institute for Research in Environmental Sciences, University of Colorado Boulder, Boulder, CO, USA

[b]now at: Chemical Sciences Division, NOAA Earth System Research Laboratory, Boulder, CO, USA

[c]now at: Department of Atmospheric and Ocean Sciences, University of Colorado Boulder, Boulder, CO, USA

Correspondence to: C. R. Thompson (chelsea.thompson@noaa.gov)

Abstract. Ozone depletion events (ODEs) in the Arctic are primarily controlled by a bromine radical-catalyzed destruction mechanism that depends on the efficient production and recycling of Br atoms. Numerous laboratory and modeling studies have suggested the importance of heterogeneous recycling of Br through HOBr reaction with bromide on saline surfaces. However, the gas-phase regeneration of bromine atoms through BrO-BrO radical reactions has been

Atmos. Chem. Phys. Discuss., doi:10.5194/acp-2015-1039, 2016
Manuscript under review for journal Atmos. Chem. Phys.
Published: 18 January 2016
© Author(s) 2016. CC-BY 3.0 License.

Atmospheric Chemistry and Physics Discussions

assumed to be an efficient, if not dominant, pathway for Br reformation and thus ozone destruction. Indeed, it has been estimated that the rate of ozone depletion is approximately equal to twice the rate of the BrO self-reaction. Here, we use a zero-dimensional, photochemical model, largely constrained to observations of stable atmospheric species from the 2009 OASIS campaign in Barrow, Alaska, to investigate gas-phase bromine radical propagation and heterogeneous recycling of bromine for a seven-day period during late March. We find that the gas-phase bromine chain length is quite small, at <1.5, and is highly dependent on ambient O_3 concentrations. As a result, ozone depletion rates estimated from only gas-phase BrO-radical reactions may significantly underestimate the rate of ozone loss. Furthermore, we find that Br atom production from primary surface emission of Br_2 and BrCl can account for between 30 – 90% of total Br atom production. This analysis suggests that heterogeneous recycling of bromine is at least as important as, and at times greater than, gas-phase recycling for the occurrence of Arctic ODEs.

1 Introduction

The springtime depletion of boundary layer ozone in the Arctic has been the subject of intense research for several decades. Early observations revealed a strong correlation between ozone depletion events (ODEs) and enhancements in filterable bromine (Barrie et al., 1988). This discovery led researchers to propose a mechanism for the bromine-catalyzed destruction of ozone.

$Br_2 + h\nu \rightarrow 2Br$ (R1)

$Br + O_3 \rightarrow BrO + O_2$ (R2)

$BrO + BrO \rightarrow Br_2 \text{ (or } Br + Br) + O_2$ (R3)

Atmos. Chem. Phys. Discuss., doi:10.5194/acp-2015-1039, 2016
Manuscript under review for journal Atmos. Chem. Phys.
Published: 18 January 2016
© Author(s) 2016. CC-BY 3.0 License.

Atmospheric Chemistry and Physics Discussions

This reaction cycle requires an initial source of bromine atoms to the boundary layer. Laboratory and theoretical studies have suggested that Br_2 could be produced through oxidation of bromide present in salt-enriched snow, ice or aerosol surfaces by gas-phase ozone (Hirokawa et al., 1998; Oum et al., 1998b; Gladich et al., 2015).

$$O_3 + 2Br^-_{(aq)} + 2H^+_{(aq)} \rightarrow\rightarrow Br_2 + O_2 + H_2O \quad (R4)$$

Field observations by Pratt et al. (2013) using a controlled snow chamber experiment with natural tundra snow collected near Barrow, AK lend further evidence to this mechanism, and also suggest Br_2 production from OH produced photochemically within the snowpack.

Once present in the gas-phase, bromine atoms can be regenerated through radical-radical reactions of BrO with XO (where X = Br, Cl, or I), NO, OH, or CH_3OO to propagate the chain reaction and continue the destruction cycle of ozone. If BrO photolyzes or reacts with NO, O_3 is regenerated, and there is a null cycle with respect to O_3; however, these two pathways represent efficient routes for Br atom propagation. Thus R3 serves to make R2 effective in destruction of O_3. At the same time, Br atoms could be recycled through heterogeneous reactions of HOBr with bromide in the condensed phase to release Br_2 to the gas-phase via the now well-known "bromine explosion" mechanism (Vogt et al., 1996; Tang and McConnell, 1996; Fan and Jacob, 1992).

$$BrO + HO_2 \rightarrow HOBr + O_2 \quad (R5)$$

$$HOBr_{(g)} \rightarrow HOBr_{(aq)} \quad (R6)$$

$$HOBr_{(aq)} + Br^-_{(aq)} + H^+_{(aq)} \leftarrow\rightarrow Br_{2(aq)} + H_2O \quad (R7)$$

$$Br_{2(aq)} \rightarrow Br_{2(g)} \quad (R8)$$

Atmos. Chem. Phys. Discuss., doi:10.5194/acp-2015-1039, 2016
Manuscript under review for journal Atmos. Chem. Phys.
Published: 18 January 2016
© Author(s) 2016. CC-BY 3.0 License.

Atmospheric Chemistry and Physics Discussions

Evidence for reaction sequence R5 – R8 has been provided through laboratory studies, which found that Br_2 was produced when frozen bromide solutions were exposed to gas-phase HOBr (Huff and Abbatt, 2002; Adams et al., 2002).

To efficiently sustain the ozone destruction cycle to the point of near complete loss of boundary layer ozone ($[O_3] < 2$ ppb), bromine atoms must be continually recycled through some combination of the above mechanisms. The gas-phase reaction cycle described by Reactions R1 – R3 has generally been considered to be the dominant pathway for Br reformation during ODEs. Thus, it has been assumed that the rate of ozone destruction can be estimated as Equation 1 (Hausmann and Platt, 1994; Zeng et al., 2006), or as Equation 2 if chlorine chemistry is considered through Reaction R9 (Le Bras and Platt, 1995; Platt and Janssen, 1995).

$$-\frac{d[O_3]}{dt} = 2 \cdot k_3 \cdot [BrO]^2 \quad (1)$$

$$-\frac{d[O_3]}{dt} = 2(k_3 \cdot [BrO]^2 + k_9 \cdot [BrO] \cdot [ClO]) \quad (2)$$

$$BrO + ClO \rightarrow Br + OClO \quad (R9)$$

However, these approximations assume that the ozone destruction rate is dominated by the BrO + XO reaction, which in turn necessitates efficient gas-phase recycling of Br; therefore, a relatively long bromine chain length would be required to account for observed rates of ozone destruction. It is, however, possible that Br atoms are generated mostly by Br_2 photolysis, followed by BrO termination, e.g. by R5, in which case a short gas-phase bromine radical chain length would be implied. The chain length for any process depends on the rates of the propagation relative to the production and destruction reactions (Kuo, 1986). In the stratosphere, the Br/BrO catalytic cycle can have a chain length ranging from 10^2 to 10^4 (Lary, 1996). In the troposphere, there is significantly less solar radiation and many more available sinks; thus, radical chain lengths can be much shorter. For example, the chain length of the tropospheric

Atmos. Chem. Phys. Discuss., doi:10.5194/acp-2015-1039, 2016
Manuscript under review for journal Atmos. Chem. Phys.
Published: 18 January 2016
© Author(s) 2016. CC-BY 3.0 License.

100 HO_x cycle has been estimated to be ~ 4 – 5 (Ehhalt, 1999; Monks, 2005), increasing to 10 – 20
101 near the tropopause (Wennberg et al., 1998). The halogen radical chain lengths in the Arctic
102 troposphere have so far not been determined, thus, it is difficult to evaluate whether Equations I
103 and II are appropriate for estimating ozone depletion rates.

104 Modeling studies using typical Arctic springtime conditions to simulate ODEs have
105 concluded that ozone depletion cannot be sustained without considering the heterogeneous
106 recycling of reactive bromine on snow or aerosol surfaces (Michalowski et al., 2000; Piot and
107 Von Glasow, 2008). Michalowski et al. (2000) determined that the rate of ozone depletion in
108 their model was limited by the mass transfer rate of HOBr to the snowpack (i.e., the rate at which
109 Br is recycled through the heterogeneous mechanism) and that the depletion of ozone is nearly
110 completely shut down when snowpack interactions are removed. Piot and von Glasow (2008)
111 simulated ozone depletion using the one-dimensional MISTRA model and concluded that major
112 ODEs (defined as complete destruction within 4 days) could only be produced if recycling of
113 deposited bromine on snow is included. Without heterogeneous recycling on the snowpack, the
114 BrO_x termination steps and irreversible loss of HOBr and HBr to the surface prohibits the
115 occurrence of an ODE. More recently, using HOBr observations from Barrow during OASIS,
116 Liao et al. (2012) found that a simple photochemical model over-predicted observed HOBr
117 during higher wind events (> 6 m s^{-1}), ostensibly due to omission of heterogeneous loss to
118 aerosol in the model, and concluded that their field observations support the hypothesis of
119 efficient recycling back to reactive bromine via this mechanism.

120 While it is evident that the reactions occurring on snow and aerosol surfaces are likely the
121 initial source of halogen species to the polar boundary layer and that heterogeneous bromine
122 recycling on these surfaces must be considered for HOBr and HBr, the relative importance of

Atmos. Chem. Phys. Discuss., doi:10.5194/acp-2015-1039, 2016
Manuscript under review for journal Atmos. Chem. Phys.
Published: 18 January 2016
© Author(s) 2016. CC-BY 3.0 License.

gas-phase versus heterogeneous recycling of Br is uncertain. The goal of this work was to investigate gas-phase Br atom propagation in terms of the bromine chain length in comparison to the production of Br atoms through heterogeneous recycling and surface emissions of Br_2 and BrCl. Here, we present results from our study using a multi-phase, zero-dimensional model constrained with time-varying measurements of molecular halogens, O_3, CO, NO, NO_2, and VOCs from the 2009 Ocean-Atmosphere-Sea Ice-Snowpack (OASIS) campaign in Barrow, Alaska. This work builds on the analysis presented in Thompson et al. (2015). By constraining our model with observations, we were able to conduct an in-depth study of the halogen atom recycling occurring under varying conditions that were observed during the campaign.

2 Experimental

2.1 Measurements and Site Description

The analysis presented herein utilizes observations conducted during the OASIS field campaign that occurred during the months of February through April of 2009 in Barrow, AK. The goal of the OASIS study was to investigate the chemical and physical processes occurring within the surface boundary layer during ozone and mercury depletion events in polar spring. This study resulted in the largest suite of simultaneous and co-located atmospheric measurements conducted in the Arctic near-surface atmosphere to date, and represents a unique opportunity for in-depth examination of a multitude of chemical interactions in this environment.

Atmospheric measurements were conducted from instrument trailers located near the Barrow Arctic Research Consortium (BARC) facility on the Naval Arctic Research Laboratory (NARL) campus. Winds arriving at the site are primarily northeasterly, from over the sea ice, and thus represent background conditions with influence from natural processes and snow-air

Atmos. Chem. Phys. Discuss., doi:10.5194/acp-2015-1039, 2016
Manuscript under review for journal Atmos. Chem. Phys.
Published: 18 January 2016
© Author(s) 2016. CC-BY 3.0 License.

Atmospheric Chemistry and Physics Discussions

146 interactions. Winds occasionally shift to westerly, bringing local emissions from the town of
147 Barrow to the site, however these isolated events are easily identifiable by coincident
148 enhancements in both NO_x and CO.

149 Measurements of molecular halogens, NO, NO_2, O_3, CO, and VOCs were used to
150 constrain the model employed in this analysis. Instrumental methods for these measurements
151 have all been described elsewhere, thus, only a brief description is provided here. Inorganic
152 halogen species (Br_2, Cl_2, BrO, and HOBr) were measured by chemical ionization mass
153 spectrometry with I^- ion chemistry as described in Liao et al. (2011, 2012, 2014); O_3, NO, and
154 NO_2 were measured by chemiluminscence (Ridley et al., 1992; Ryerson et al., 2000). CO was
155 measured using a standard commercial CO analyzer (Thermo Scientific) with infrared absorption
156 detection, and formaldehyde (HCHO) was measured at 1 Hz frequency using a tunable diode
157 laser absorption spectrometer, as described in Fried et al. (1997) and Lancaster et al. (2000). A
158 large suite of organic compounds was measured in situ by fast GC-MS (Apel et al. 2010) and via
159 whole air canister samples with offline GC-MS (Russo et al., 2010).
160

161 **2.2 Model Description**

162 The model used for this study is a multi-phase, zero-dimensional box model developed
163 using the commercial software FACSIMILE. A detailed description of the model can be found
164 in Thompson et al. (2015). We will describe the model only briefly here.

165 Our model consists of 220 gas-phase reactions and 42 photolysis reactions, representing
166 much of the known gas-phase chemistry occurring in the Arctic, including the important halogen,
167 HO_x, NO_x and VOC chemistry associated with ozone depletions. The model also includes an
168 inorganic iodine reaction scheme adapted from McFiggans et al. (2000, 2002), Calvert and

Atmos. Chem. Phys. Discuss., doi:10.5194/acp-2015-1039, 2016
Manuscript under review for journal Atmos. Chem. Phys.
Published: 18 January 2016
© Author(s) 2016. CC-BY 3.0 License.

Atmospheric Chemistry and Physics Discussions

169 Lindberg (2004) and Saiz-Lopez et al. (2008). Although IO has not been unambiguously
170 measured in the High Arctic above the ~1.5 – 2 pptv detection limit of LP-DOAS (long-path
171 differential optical absorption spectroscopy), observed enhancements in filterable iodide and
172 total iodine suggest that iodine chemistry is active to some extent in this region (Sturges and
173 Barrie, 1988; Martinez et al., 1999; Mahajan et al., 2010; Hönninger, 2002). Recently, I_2 has
174 been detected at tens of pptv within the snowpack interstitial air near Barrow, AK and at ≤0.5
175 pptv in the near surface air by I^- CIMS, providing direct evidence supporting the presence of at least low
176 levels of iodine chemistry (Raso et al., 2015). Here, we investigate the impact of two different levels
177 of iodine, referred to hereafter as "Low Iodine" and "High Iodine" in certain modeling
178 simulations by introducing a flux of I_2. For the Low Iodine case, the I_2 flux was chosen such that
179 average daytime mole ratios of IO remain near 1 pptv for the majority of the simulation. The
180 High Iodine scenario incorporates a flux that is adjusted such that I_2 averages 0.5 pptv across the
181 simulated period. This results in IO mole ratios ranging from 5 to 10 pptv.

182 All gas-phase rate constants used in this model were calculated for a temperature of 248
183 K, consistent with ambient conditions in Barrow for the period simulated. Table 1 contains an
184 abbreviated list of the reactions included in the model, showing only those reactions that are
185 central to the production, propagation, and termination of bromine radical chemistry that is the
186 focus of this study. A complete list of reactions can be found in Thompson et al. (2015).

187 The model is configured to simulate 7 days during late March, 25 through 31 March, that
188 include a period of depleting ozone, a full ozone depletion ($[O_3] < 2$ ppbv) lasting ~ 3 days, and
189 recovery. The O_3 time-series for this period is shown in Figure 1, along with radiation as a
190 reference (all plots are in Alaska Standard Time). We constrain the model to observations for
191 this time period by reading in time-varying data sets of O_3, C_2H_2, C_2H_4, C_2H_6, C_3H_8, C_3H_6, *n*-
192 C_4H_{10}, *i*-C_4H_{10}, HCHO, CH_3CHO, CH_3COCH_3, methyl ethyl ketone (MEK), Cl_2, Br_2, NO, NO_2,

Atmos. Chem. Phys. Discuss., doi:10.5194/acp-2015-1039, 2016
Manuscript under review for journal Atmos. Chem. Phys.
Published: 18 January 2016
© Author(s) 2016. CC-BY 3.0 License.

and CO at ten-minute time steps. All other gas-phase species are allowed to freely evolve. Surface fluxes (represented as volumetric fluxes) are used for HONO and I_2 and are scaled to $J(NO_2)$ as a proxy for radiation as both of these species are likely to be produced photochemically. Further discussion regarding HONO can be found in Thompson et al. (2015).

Photolysis rate constants (J coefficients) for many of the species included were calculated during OASIS using the Tropospheric Ultraviolent and Visible Radiation model from measurements of down-welling actinic flux conducted throughout the campaign (Shetter and Müller, 1999; Stephens et al., 2012). Estimates of J_{max} in the Arctic for OClO were taken from Pöhler et al. (2010) and for HOCl from Lehrer et al. (2004). J_{max} values for the iodine compounds were calculated according the work of Calvert and Lindberg (2004), which also simulated conditions for late March in Barrow, Alaska. Time-varying J coefficients for O_3 and NO_2 were read into the model at 10-minute time steps and all other photolysis reactions were scaled to $J(NO_2)$ in the modeling code.

Heterogeneous reactions of halogen species occurring in aerosol and in the snowpack are also included, as well as mass transfer and dry deposition for certain species using the method and mechanism of Michalowksi et al. (2000). It was intended to utilize strictly multiphase chemistry to produce halogen radical precursors using this mechanism, however, the heterogeneous production mechanisms could not reproduce observed Br_2 or Cl_2 from OASIS. This likely reflects the complex but not fully understood condensed phase chemistry and physics that leads to production of Br_2 (and Cl_2) (Pratt et al., 2013). Thus, Br_2 and Cl_2 concentrations were fixed at the observed levels (see Thompson et al., 2015 for further discussion). Only daytime BrCl was used as produced in the model multiphase mechanism. BrCl measurements from OASIS are sparse, however, the daytime simulated BrCl mole ratios of 0 – 10 pptv are in

Atmos. Chem. Phys. Discuss., doi:10.5194/acp-2015-1039, 2016
Manuscript under review for journal Atmos. Chem. Phys.
Published: 18 January 2016
© Author(s) 2016. CC-BY 3.0 License.

approximate agreement with the available data for the campaign. BrCl was not a significant source of either Br or Cl atoms relative to Br_2 and Cl_2.

The dry deposition velocity of O_3 to the snowpack is estimated at 0.05 $cm \cdot s^{-1}$, consistent with previous measurements and modeling studies (Gong et al., 1997; Michalowski et al., 2000; Helmig et al., 2007; Cavender et al., 2008), though it is recognized that there is large uncertainty with this parameter from field observations (Helmig et al., 2007, 2012). Assuming a boundary layer height of 300 m, this corresponds to a transfer coefficient, k_t, of 1.67×10^{-6} s^{-1}. Dry deposition velocities for the stable Arctic environment have not been determined for the halogen acids (HBr, HCl, HOBr, HOCl, HOI), therefore we use the estimation method of Michalowski et al. (2000) and assume a deposition velocity that is 10 times greater than for O_3, leading to a k_t of 1.67×10^{-5} s^{-1}. We assume an equivalent k_t for the oxidized nitrogen compounds (HNO_3, HO_2NO_2, HONO, and N_2O_5). The rate of transfer out of the snowpack of emitted species, assumed here to be limited only by vertical mixing, is estimated as 1.67×10^{-5} s^{-1}, or equivalent to the rate of deposition of the halogen acids (Michalowski et al., 2000). This is chosen as a best estimate of vertical mixing because the deposition of halogen acids is likely to be only limited by the rate of vertical mixing. The mass transfer coefficient of atmospheric species to and from the particle phase is calculated as a first-order process as described in Jacob (2000).

3 Results and Discussion

3.1 Comparison of modeled and observed Br_2, BrO, HOBr, and HO_2

This work focuses on the propagation and production mechanisms of Br atoms, and thus it is critical that our model accurately simulates BrO and Br_2 at mole ratios that are consistent with observations. Figures 2A and 2B show comparisons between simulated mole ratios (black

Atmos. Chem. Phys. Discuss., doi:10.5194/acp-2015-1039, 2016
Manuscript under review for journal Atmos. Chem. Phys.
Published: 18 January 2016
© Author(s) 2016. CC-BY 3.0 License.

trace) of Br_2 and BrO compared to the measured values during this time (red data) by chemical ionization mass spectrometry (CIMS) (Liao et al., 2012b). In the model, Br_2 is fixed to time-varying observations, whereas BrO is produced strictly through the gas-phase photochemical reactions. The model captures the overall temporal profile and magnitude of BrO throughout the period. It should be noted, however, that the uncertainty in the BrO measurements is high during ODEs as the observed values are very near the detection limit (LOD of ~2 pptv with uncertainty of -3/+1 pptv near the LOD). Simulated Br_2 reaches up to 2 – 12 pptv (Figure 2A) during the daytime resulting from the large surface fluxes that in turn produce the BrO mole ratios observed. These Br_2 levels are consistent with previous Arctic measurements that observed daytime Br_2 up to 27 pptv (Foster et al., 2001) and agree well with the "uncorrected" Br_2 data reported in Liao et al. (2012a, 2012b) for this period. It has been suggested that daytime Br_2 higher than the CIMS instrumental detection limit (~1 pptv) is an artifact of HOBr conversion to Br_2 on the instrument inlet (Neuman et al., 2010), however, for the instrument configuration employed during OASIS, it is not clear how much, if any, of the Br_2 signal is a result of HOBr reactions on instrument surfaces. An estimate of the effective mixing height of Br_2 can be calculated using the method of Guimbaud et al. (2002) and using an average measured diffusivity during OASIS of 1500 $cm^2\ s^{-1}$ (R. Staebler, personal communication, 2015). By assuming that photolysis is the dominant loss mechanism controlling the Br_2 mid-day lifetime in a stable boundary layer typical of Arctic conditions, the daytime effective mixing height is ~1.85 m. Therefore, the majority of the Br_2 present at the surface (the likely source of emission) would remain at the height of the instrument inlet (~1 m) in the sunlit periods. In our highly constrained model, daytime Br_2 mole ratios greater than 1 pptv are necessary to reproduce observed BrO, therefore, this modeling study

Atmos. Chem. Phys. Discuss., doi:10.5194/acp-2015-1039, 2016
Manuscript under review for journal Atmos. Chem. Phys.
Published: 18 January 2016
© Author(s) 2016. CC-BY 3.0 License.

suggests that Br_2 should indeed be present and above the instrument detection limit during the daytime.

Overall, the model captures the temporal cycle of HOBr well, but often overpredicts daytime maximum mole ratios (Figure 2C). A case in point is the much higher than observed HOBr levels on 31 March, which corresponds to a similar overprediction of BrO. Observed Br_2 is relatively high on this day, and given that the model is forced to these observations, if the high Br_2 is due to instrument artifact of HOBr conversion on the inlet, this could account for the model discrepancy here.

HO_2 is essential for the heterogeneous recycling of bromine (via Reactions R5 – R7). Therefore, it is important that our model accurately simulates HO_2 for this analysis. In Figure 2D we show a comparison of simulated HO_2 (black trace) and observed HO_2 from OASIS for this period (red data), measured using a CIMS developed for peroxy radicals (Edwards et al., 2003). Our model captures the diurnal cycle of HO_2 and the daily fluctuations observed. Simulated HO_2 is on the lower limit of observations for 29 March, and does not reach the maximum mole ratios observed. The model also slightly overpredicts HO_2 on 28 and 30 March, though is within the range of uncertainty of the measurement.

3.2 Chain length

The ozone destruction cycle as described in Reactions R1 – R3 is a chain reaction mechanism catalyzed by BrO_x. The effectiveness of a catalytic cycle can be can be quantified by considering the chain length, that is, the number of free radical propagation cycles per termination or per initiation. We have not, until the OASIS2009 campaign, had the high quality

Atmos. Chem. Phys. Discuss., doi:10.5194/acp-2015-1039, 2016
Manuscript under review for journal Atmos. Chem. Phys.
Published: 18 January 2016
© Author(s) 2016. CC-BY 3.0 License.

Atmospheric Chemistry and Physics Discussions

283 measurements available to enable a reliable estimation of the bromine radical chain length in the
284 Arctic.

285 The length of the chain in a radical propagation cycle is limited by termination steps that
286 destroy the chain carriers and result in relatively stable atmospheric species. Thus, the chain
287 length can be defined as the rate of propagation divided by the rate of termination. Alternatively,
288 the chain length can also be calculated using the rate of initiation. If the total bromine radical
289 population is at steady-state, the rate of initiation is equal to the rate of termination; thus, for
290 short-lived radical species, the two methods for calculating chain length should be approximately
291 equal.

292 Method 1: $$\Phi = \frac{\Sigma(\text{Rates of propagation})}{\Sigma(\text{Rates of termination})} \quad (3)$$

293 Method 2: $$\Phi = \frac{\Sigma(\text{Rates of propagation})}{\Sigma(\text{Rates of initiation})} \quad (4)$$

294 We used our model to calculate the chain length for bromine radical propagation across
295 the 7-days of the simulated period using both Method 1 and 2 as shown in Equations 5 and 6.
296 Because bromine radicals are generated photolytically, the chain length is calculated for daytime
297 only, defined here as approximately 7:00 to 20:00 Alaska Standard Time (AKST).

298

299 Method 1: $$\Phi_{Br} = \frac{\begin{array}{l}(2k[BrO]^2 + J_{BrO}[BrO] + J_{BrONO2}[BrONO_2] + \\ k[BrO][ClO] + k[BrO][IO] + k[BrO][CH_3OO] + \\ k[BrO][OH] + k[BrO][O(^3P)] \\ + k[BrO][CH_3COOO] + k[BrO][NO])\end{array}}{\begin{array}{l}(k[Br][HO_2] + k[Br][C_2H_2] + k[Br][C_2H_4] \\ + k[Br][C_3H_6] + k[Br][HCHO] + k[Br][NO_2] \\ + k[Br][CH_3CHO] + k[Br][C_3H_6O] + k[Br][C_4H_8O] \\ + k[Br][CH_3OOH] + k[BrO][HO_2] + k[BrO][CH_3OO] \\ + k[BrO][C_3H_6O] + k[BrO][NO_2])\end{array}} \quad (5)$$

308
309
310
311

Atmos. Chem. Phys. Discuss., doi:10.5194/acp-2015-1039, 2016
Manuscript under review for journal Atmos. Chem. Phys.
Published: 18 January 2016
© Author(s) 2016. CC-BY 3.0 License.

Atmospheric Chemistry and Physics Discussions

Method 2:

$$\Phi_{Br} = \frac{(2k[BrO]^2 + J_{BrO}[BrO] + J_{BrONO2}[BrONO_2] + k[BrO][ClO] + k[BrO][IO] + k[BrO][CH_3OO] + k[BrO][OH] + k[BrO][O(^3P)] + k[BrO][CH_3COOO] + k[BrO][NO])}{(2J_{Br2}[Br_2] + J_{BrCl}[BrCl] + J_{HOBr}[HOBr] + J_{IBr}[IBr] + k[CH_3Br][OH] + k[CHBr_3][OH])} \quad (6)$$

Termination reactions for bromine include those reactions that are sinks for either Br and BrO, since Br and BrO rapidly interconvert. Here, photolysis of BrO and the BrO + NO reaction is included in the numerator because they are efficient at reforming Br and propagating the chain; however, these reactions do not result in a net loss of ozone. Photolysis of BrO produces atomic oxygen that reacts with O_2 to form O_3, and NO_2 can photolyze to similarly reform O_3. Therefore, it should be noted that if we omit these reactions and consider only those that result in a net O_3 loss, it would be expected that the chain length would be shorter. Indeed, model simulations were performed without these two terms and the determined chain lengths were on average 80% lower than those presented here. BrO reaction with CH_3OO is included in both the numerator and denominator in Equation 5 because this reaction has two channels, one that propagates the Br chain and one that terminates it.

In Figure 3, we present the results of these calculations for the Base Model, which show that the two methods for calculating bromine chain length are in reasonably good agreement, although there are small differences between the two methods throughout the time-series. This agreement is a test of our basic understanding of the radical chemistry. The inset graph in Figure 3 shows a linear regression of the two methods for the chain length calculation. The coefficient of determination (r^2) of 0.79 confirms the good temporal agreement between the two methods; however, the slope of 0.72 indicates that Method 1 is generally higher than Method 2 throughout (with some periods of exception). This offset reveals that either Method 1 is slightly

Atmos. Chem. Phys. Discuss., doi:10.5194/acp-2015-1039, 2016
Manuscript under review for journal Atmos. Chem. Phys.
Published: 18 January 2016
© Author(s) 2016. CC-BY 3.0 License.

overestimating the chain length, or that Method 2 is underestimating it. The numerator is identical in Equations 5 and 6, therefore, the denominator must be driving this discrepancy, with either the denominator term in Method 1 too low or the denominator term in Method 2 too high (or some combination thereof). If it's the case that the Method 1 denominator is too low, then it must be concluded that there are important BrO_x sink terms that are missing from the calculation. If, however, the denominator of Method 2 is too high, this would imply that our measurements of these BrO_x precursors are too high, which, as discussed above, is a known likelihood at least for the Br_2 measurements.

In Equation 6, we also do not include photolysis of organobromine compounds because the rate of Br atom production from this pathway is small (e.g., ~ 100 molecules·cm^{-3}·s^{-1} for bromoform at mid-day) compared to Br atom production from Br_2 photolysis (~1.3x10^7 molecules·cm^{-3}·s^{-1} at mid-day assuming 5 pptv of Br_2). Photolysis of bromine nitrate ($BrONO_2$) is included, however, the prevalence of and production of this compound in the Arctic is highly uncertain, and no observations of this species in the Arctic have been published to date with which to compare to our modeled mole ratios. Inclusion of this term at the modeled $BrONO_2$ mole ratios has negligible effect on the calculated chain length. The sum of the rates of Br atom production from all possible organobromine compounds (and potentially greater levels of $BrONO_2$ or other bromine-NO_y species) combined may help account for the slight discrepancy between the two methods for calculating the bromine chain length, at least for cases where Method 2 yields larger chain lengths. This may be part of the explanation for the small grouping of data points in the inset graph of Figure 3, colored in red, that display abnormally high chain lengths via Method 2 but quite low chain lengths using Method 1. These points correspond to the morning of 25 March, a short period of anthropogenic pollution when NO_x (and NO_y) were

Atmos. Chem. Phys. Discuss., doi:10.5194/acp-2015-1039, 2016
Manuscript under review for journal Atmos. Chem. Phys.
Published: 18 January 2016
© Author(s) 2016. CC-BY 3.0 License.

361 exceptionally high (Thompson et al., 2015). Thus, the BrO + NO_2 and Br + NO_2 sink terms in
362 Method 1 become dominant for this period, significantly shortening the calculated chain length.
363 Because of this high NO_x chemistry, it is likely that bromine-NO_y species would be an important
364 production term in Method 2 during this period.

365 Overall, the median bromine chain-length in the Base simulation is ~1.3 across daylight
366 hours (7:00 to 21:00 AKST) and ~2 for mid-day, defined for this purpose as approximately 12:00
367 until 18:00 AKST, when $[O_3] \geq 5$ ppbv. In comparison, the bromine chain length is ~0.3 when
368 $[O_3] < 5$ ppbv (Figure 3). In other words, the chain cannot be maintained when $[O_3] < 5$ ppbv.
369 Often there is an early morning enhancement in the chain length, such as on 25 and 29 March.
370 These morning spikes appear to correlate with a similar sharp increase in ozone. Br_2
371 accumulates during the nighttime hours, resulting in the highest Br_2 concentrations in the early
372 morning hours (Figure 2B). When the sun rises, Br_2 photolyzes rapidly, releasing a pulse of
373 reactive bromine that converts to BrO in the presence of ozone. This, in concert with the
374 coincident increases in ozone on these days, can explain the enhanced chain lengths during the
375 early morning hours.

376 Overall, midday bromine chain lengths remain near or below 2 during background O_3
377 days. This implies that, for these days, ozone depletion is strongly dependent upon initiation
378 processes, and most BrO radicals produced terminate the chain via reactions R5 and R10 in less
379 than two cycles. Reaction R12 will also efficiently terminate the chain, however, the relative
380 importance of R10 and R12 depend upon the relative abundances of BrO and Br. For background
381 O_3 days, such as 29 and 30 March, [BrO] > [Br], thus, R10 > R12. The low chain lengths
382 calculated here are surprising, given that it has been generally accepted that Br is recycled
383 efficiently in the gas-phase. That it appears this is not the case suggests that heterogeneous

Atmos. Chem. Phys. Discuss., doi:10.5194/acp-2015-1039, 2016
Manuscript under review for journal Atmos. Chem. Phys.
Published: 18 January 2016
© Author(s) 2016. CC-BY 3.0 License.

recycling through the "bromine explosion", which emits Br_2 and BrCl from surface reactions, must be of critical importance for ODEs occurring at the surface, as was previously concluded by Piot and von Glasow (2008) and Michalowski et al. (2000).

A question to address regarding the relatively small chain length calculated for Br is to what extent the chain length is dependent on NO_2. As discussed in Thompson et al. (2015) and further investigated in Custard et al. (2015), NO_2 at Barrow can be greater and more variable than at very remote sites due to its proximity to anthropogenic emissions sources. We find that the chain length calculation is relatively insensitive to NO_2 concentrations and so it is robust for the range of conditions encountered at Barrow. As discussed in Custard et al. (2015), while NO_2 can inhibit the bromine chain through reactions R10 and R12 (i.e., decreasing the chain length), enhanced NO_2 will also reduce available HO_2, thereby decreasing the HO_2 available to terminate the chain (i.e., increasing the chain length). While the Method 2 calculation does not contain NO_2 in the denominator, the absolute [BrO] is NO_x-dependent because of reaction R10 (Custard et al., 2015). Br_2 production can potentially also be NO_x-dependent, e.g. via reaction R11, followed by R7.

$$BrO + NO_2 \rightarrow BrONO_2 \quad \text{(R10)}$$

$$BrONO_{2(aq)} + H_2O \rightarrow HOBr + HNO_3 \quad \text{(R11)}$$

$$Br + NO_2 \rightarrow BrNO_2 \quad \text{(R12)}$$

However, for the period March 26 - March 30, NO_x was relatively low, and the relatively good agreement between the two calculation methods further supports our conclusion.

To investigate how chemical interactions with chlorine and iodine affect the bromine chain length, a series of simulations was performed by varying the combinations of halogens present in the model. The bromine chain length was determined for scenarios with only Br, Br

Atmos. Chem. Phys. Discuss., doi:10.5194/acp-2015-1039, 2016
Manuscript under review for journal Atmos. Chem. Phys.
Published: 18 January 2016
© Author(s) 2016. CC-BY 3.0 License.

and Cl (Base Model), Br and Low Iodine, Br and High Iodine, Base with Low Iodine, and Base with High Iodine. Simulations without chlorine were performed simply by removing Cl_2, while simulations with iodine were performed by incorporating the I_2 flux as described in Section 2.2. No other adjustments were made to the model for these sensitivity runs.

Table 2 shows the results for both chain length calculation methods (i.e., Equations 5 and 6) for the different halogen combinations for the three days when ozone was present near background values: 25, 29 and 30 March. For the Base scenario ("Br and Cl"), the average bromine chain length is 1.13 – 1.41 (considering the two different calculation methods). In comparison with the "Br Only" run, Cl chemistry does not induce a net increase in the Br chain length, but rather causes a slight decrease, though this is not a significant decrease given the ranges for the two calculation methods. Cl chemistry can increase Br radical propagation through the addition of the BrO + ClO cross-reaction and enhancement of the BrO + CH_3OO radical propagation terms. However, Cl chemistry can also increase the concentration of reactive bromine sinks, such as aldehydes (e.g., propanal and butanal, which were free to evolve in our model; HCHO and CH_3CHO are fixed to observations) and HO_2 (see Thompson et al., 2015). Iodine has a larger effect on the Br chain length. When Low Iodine is added to the "Br Only" simulation, the chain increases from 1.17 – 1.51 to 1.21 – 1.67, primarily due to the very fast cross-reaction between IO and BrO. Interestingly, there is no significant difference in the calculated chain length between the "Br and Low Iodine" and the "Br and High Iodine" simulations, potentially due to the increased competition for NO by I atoms. The addition of Cl to the "Br and I" simulation imparts a slight decrease to the Br chain length. This may be explained by the competition between BrO and ClO for reaction with NO and/or IO, as well as the additional Br sinks in the presence of Cl chemistry. Regardless, overall there is more Br

Atmos. Chem. Phys. Discuss., doi:10.5194/acp-2015-1039, 2016
Manuscript under review for journal Atmos. Chem. Phys.
Published: 18 January 2016
© Author(s) 2016. CC-BY 3.0 License.

available for reaction with O_3 when Cl is present due to the interhalogen reactions, thereby increasing the rate of ozone depletion (see Thompson et al., 2015 for further discussion on ozone depletion rates).

There are several conclusions that can be drawn from Figure 3 and Table 2: 1) there is a distinct difference in bromine chain length between O_3-depleted and non-depleted days with a significantly larger chain length when ozone is present, and 2) for all simulations, the average bromine chain is much shorter than expected (given that gas-phase recycling has, to date, been assumed to be highly efficient). The chain length is greatest when ozone is present because many of the species that propagate the Br chain (e.g., BrO, ClO, IO, and to a lesser extent OH and CH_3OO) require O_3 for production. Although the relationship between bromine chain length and BrO is not straightforward due to the multitude of interactions between BrO and other species that either propagate or terminate the chain, the chain length does exhibit a rough dependence on [BrO], shown in Figure 4, that can be loosely described with a linear fit. If it were the case that the gas-phase Br chain length was relatively long (such that the numerator far outweighs the denominator), and dominated by the BrO self-reaction, the numerator in Equations 5 and 6 would reduce to $2k[BrO]^2$, and the regression in Figure 4 would display a quadratic fit; however, that is not observed here.

For purposes of comparison, the chain lengths for Cl and I were also calculated in a manner analogous to that of Equation 5. These results are shown in Figure 5 for the Base + Low Iodine scenario. It is apparent from this figure that reactive Cl exhibits an exceptionally short chain length, whereas reactive I has a relatively long chain length. The average Cl chain length across the three days of background ozone (25, 29, and 30 March) is 0.15, or 0.23 considering only mid-day hours (12:00 – 18:00 AKST). This result indicates that nearly all Cl atoms that are

Atmos. Chem. Phys. Discuss., doi:10.5194/acp-2015-1039, 2016
Manuscript under review for journal Atmos. Chem. Phys.
Published: 18 January 2016
© Author(s) 2016. CC-BY 3.0 License.

453 produced terminate, likely through the very efficient reaction with a multitude of VOCs, as
454 shown in Thompson et al. (2015). This behavior also explains why Cl has only a small effect on
455 the bromine chain length. In contrast, I and IO have few known sinks, which results in a reactive
456 iodine chain length of 5.84 on average over 25, 29, and 30 March, and 7.44 over only mid-day
457 hours, with maxima over 15. The high efficiency of the gas-phase regeneration of I in part
458 explains why iodine is more efficient on a per atom basis at depleting ozone than either Br or Cl
459 (Thompson et al., 2015).
460
461 **3.3 Reactive bromine termination and propagation pathways**
462 The individual reactions that propagate and terminate the reactive bromine chain were
463 examined to determine the most important reaction pathways. The rates of reaction of these
464 propagation pathways over the 7-day period, with and without iodine, are shown in Figure 6 A
465 and B. The y-axes are expressed as the cumulative rate of reaction. The rate of the BrO + BrO
466 reaction is calculated as $2k[BrO]^2$, since this reaction results in the production of two Br atoms.
467 From this plot, it is apparent that the reaction pathways that dominate the bromine propagation,
468 i.e., BrO photolysis and reaction with NO, are those that do not result in a net ozone loss. This is
469 an important result in that it suggests that much of the time BrO regenerates Br without a net loss
470 of ozone for the simulated conditions in Barrow. Indeed, in our previous paper, we calculated
471 that ~70% of gas-phase BrO reforms ozone via photolysis or reaction with NO over this period
472 (Thompson et al., 2015). The inset pie charts, which show the average fractional importance of
473 the various propagation reactions for 29 and 30 March, reveal that these two pathways account
474 for 84 – 91% of the total. Interestingly, the BrO self-reaction is small in comparison, with an
475 average contribution of 5 – 6%, and a maximum of 46%. However, if we consider only those

Atmos. Chem. Phys. Discuss., doi:10.5194/acp-2015-1039, 2016
Manuscript under review for journal Atmos. Chem. Phys.
Published: 18 January 2016
© Author(s) 2016. CC-BY 3.0 License.

Atmospheric Chemistry and Physics Discussions

reactions that *do* lead to a net ozone loss, then the BrO self-reaction accounts for an average of 71% and a maximum of 98% of the propagation. The rate of the BrO + ClO reaction rate is much smaller than that for BrO + BrO, though not insignificant. While on average this reaction pathway accounts for only 2%, it does reach 16% when Cl_2 is high on 29 March. In considering only those reactions that result in a net ozone loss, the BrO + ClO pathway accounts for 21% on average, and up to a maximum of 57%. In Panel B, the Base + High Iodine scenario is shown. At these levels, the BrO + IO reaction is more important than even BrO + BrO, accounting for 8% on average and a maximum of 39%. In the Base + Low Iodine scenario (not shown), the BrO + IO reaction contributes 4%, which is at times comparable to BrO + BrO and greater than BrO + ClO, even at the low IO concentrations in this simulation (~1 pptv).

The short gas-phase chain length calculated for bromine propagation indicates that there are large reactive bromine (BrO_x) sinks terminating the chain reaction. Figure 7 presents the rates of the most important BrO_x termination reactions, with the y-axis expressed as the cumulative rate of reaction. Here it can be seen that reaction of BrO with NO_2 is the dominant sink for BrO_x on non-ODE days for the conditions encountered at Barrow, while Br reaction with CH_3CHO is most important when O_3 is depleted. That HO_2 is a significant sink, and would be more so in less anthropogenically-impacted Polar Regions, points toward the importance of heterogeneous recycling through the bromine explosion mechanism. During ozone depletion, such as the major event from days 26 – 28 March ($[O_3] < 5$ppbv) when BrO is mostly absent, CH_3CHO becomes the primary sink term for Br, and HCHO is relatively more important. The strength of the CH_3CHO sink is much greater than is HCHO, as noted previously by Shepson et al. (1996). Of note are the relatively similar magnitudes of the total rate of reaction of the propagation and termination reactions shown in Figures 6 and 7, respectively, which of course

Atmos. Chem. Phys. Discuss., doi:10.5194/acp-2015-1039, 2016
Manuscript under review for journal Atmos. Chem. Phys.
Published: 18 January 2016
© Author(s) 2016. CC-BY 3.0 License.

Atmospheric Chemistry and Physics Discussions

must be the case for a chain length near 1. This accounts for the short bromine chain length determined here. This also implies then that to sustain elevated bromine radical concentrations necessary to deplete O_3 requires an equally large Br_2 source (initiation) term, likely in the form of a significant surface Br_2 flux.

3.4 Ozone loss rate

Since the chain length calculations seem to suggest a larger than expected contribution of heterogeneous bromine recycling to Br atom production, to examine this further, we calculated the rate of net ozone loss by Br and Cl in the Base Model using Equation 7 and compared this rate to that estimated by Equation 2 (Platt and Janssen, 1995; Le Bras and Platt, 1995). Additionally, the total simulated chemical ozone loss in the Base Model was calculated from Equation 8, which includes O_3 destruction by OH, HO_2, and photolysis (determined here as $k[O(^1D)][H_2O]$).

$$O_3 \text{ Loss by Br and Cl} = (k[Br][O_3] - J[BrO] - k[BrO][NO]) + (k[Cl][O_3] - J[ClO] - k[ClO][NO]) \quad (7)$$

$$\text{Total Chemical } O_3 \text{ loss rate} = k[Br][O_3] + k[Cl][O_3] + k[O(^1D)][H_2O] + k[OH][O_3] + k[HO_2][O_3] - k[BrO][NO] - J[BrO] - k[ClO][NO] - J[ClO] \quad (8)$$

The method in Equation 2 assumes that the rate of ozone loss is equivalent to the rate at which Br is regenerated through BrO reaction with itself and ClO (thus assuming efficient gas-phase propagation and a long chain length), whereas Equation 7 accounts for all net ozone destruction by Br and Cl, by correcting for those reactions that release a triplet oxygen atom and reform O_3. In other words, this method accounts for the fact that some BrO radicals react to terminate the chain (and at steady state, an equivalent BrO_x production rate is necessary). Figure 8A compares these two estimations for O_3 loss rate in the green trace (Equation 2) and the pink trace (Equation

Atmos. Chem. Phys. Discuss., doi:10.5194/acp-2015-1039, 2016
Manuscript under review for journal Atmos. Chem. Phys.
Published: 18 January 2016
© Author(s) 2016. CC-BY 3.0 License.

Atmospheric Chemistry and Physics Discussions

524 7). This comparison clearly shows that there is a large difference between the methods, with the
525 estimation from Equation 2 significantly smaller overall. Additionally, the total chemical O_3 loss
526 (calculated by Equation 8) is shown in the dashed black trace. The O_3 loss rate estimation
527 presented in Equation 7 accounts for nearly all of chemical O_3 loss (i.e., most chemical O_3 loss is
528 a result of halogen chemistry), such that the pink trace lies almost completely on top of the black
529 trace. A regression of the two estimation methods shown in Equations 2 and 7 versus the total
530 chemical O_3 loss rate (Equation 8) is presented in Figure 8B. Here it can be seen from the pink
531 data that halogen chemistry accounts for 99% of the total chemical O_3 loss under the conditions
532 simulated here. Importantly, the O_3 loss rate estimation presented in Equation 2 accounts for
533 only 44% of the total chemical O_3 loss rate (shown as the green data in Figure 8B). This
534 quantitatively expresses the conclusion that the gas-phase recycling of bromine is not as efficient
535 as previously considered and that it is often the case, for Barrow, that BrO_x terminations must
536 often, through reactions R5 or R10, be followed by heterogeneous production of Br_2 through
537 condensed-phase reactions of HOBr and/or $BrONO_2$. Indeed, the two methods for estimating
538 ozone loss rate agree the most when BrO, and thus, the gas-phase chain length are the greatest, or
539 in other words, when the $2k[BrO]^2$ term, present in both Equations 2 and 5, is most important. A
540 very significant conclusion from this analysis is that the chemical O_3 loss rate is largely
541 underestimated when calculated from only BrO observations using the $2(k[BrO]^2 + [BrO][ClO])$
542 method. This may have significant impacts on the process of examining ODEs and addressing
543 the extent to which they represent local scale chemistry versus transport effects. While this
544 situation is significantly impacted by local NO_x sources at Barrow, NO_x is expected to increase
545 with development around the Arctic.
546

Atmos. Chem. Phys. Discuss., doi:10.5194/acp-2015-1039, 2016
Manuscript under review for journal Atmos. Chem. Phys.
Published: 18 January 2016
© Author(s) 2016. CC-BY 3.0 License.

Atmospheric Chemistry and Physics Discussions

3.5 Bromine atom production

If it is the case that heterogeneous recycling is of such importance, it may be that Reaction R5 (BrO + HO_2) competes favorably with Reaction R3 (BrO + BrO). Panel A of Figure 9 shows the rates of reactions R5 and R3. This plot demonstrates that the rate of reaction of BrO with HO_2 is often of a comparable or greater magnitude than the BrO self-reaction, and remains significant throughout the simulated period. Because the BrO + HO_2 reaction is of primary importance for the bromine explosion mechanism, this result supports the hypothesis that heterogeneous recycling may be equally or even more important than gas-phase recycling of reactive bromine.

Given that the chain length is small, it must be that initiation is an important source of Br atoms. To further examine the question of surface emissions versus gas-phase recycling, we determined the rate of production of Br atoms via photolysis of Br_2 and BrCl (Equation 9), as both are emitted from the surface as products of the bromine explosion, compared to the rate of production of Br atoms through gas-phase recycling calculated by Equation 10.

$$\textit{Br Production from Surface Emissions} = 2 \times J_{Br2}[Br_2] + J_{BrCl}[BrCl] \quad (9)$$

$$\begin{aligned}\textit{Gas-phase Br Production via Recycling} = {} & 2k[BrO][BrO] + k[BrO][ClO] \\ & + k[BrO][NO] + k[BrO][OH] + k[BrO][O(^3P)] \\ & + k[BrO][CH_3OO] + k[BrO][CH_3COOO] \\ & + J_{HOBr}[HOBr] + J_{BrO}[BrO] + J_{BrONO2}[BrONO_2]\end{aligned} \quad (10)$$

Panel B of Figure 9 compares the results of Equations 9 and 10, showing the total rate of Br atom production separated into primary Br production (purple) and gas-phase Br regeneration (orange); Panel C plots the fraction of total Br atom production that is due to primary production from Br_2 and BrCl emissions. The majority of the time during this 7-day period Br atom production from Br_2 and BrCl emissions (Equation 9) accounts for 40% or greater of the total, and at times reaches over 90%. This explains both how ozone depletion can be rapid despite the

Atmos. Chem. Phys. Discuss., doi:10.5194/acp-2015-1039, 2016
Manuscript under review for journal Atmos. Chem. Phys.
Published: 18 January 2016
© Author(s) 2016. CC-BY 3.0 License.

short calculated bromine radical chain length, as well as the difference found between the two methods of estimating O_3 loss rate in Figure 7. It can be concluded from this analysis, then, that the heterogeneous recycling of bromine can be of equal or greater importance to the evolution of ODEs than gas-phase Br regeneration through radical recycling reactions.

4 Conclusions

The analysis presented here suggests that the gas-phase recycling of bromine species may be less important than commonly believed, and we conclude that heterogeneous recycling, primarily through the snowpack, is critical for the evolution of ODEs/AMDEs, consistent with results by Piot and von Glasow (2008) and Michalowski et al. (2000). Indeed, the gas-phase bromine propagation chain length is much shorter than expected, suggesting that much of the Br present in the gas-phase is primary Br from surface emissions. Again note that our calculation of chain length includes photolysis of BrO and BrO + NO, which do not result in net O_3 loss. Had we omitted these two reactions, which we have found are in fact dominating the radical propagation, the chain length would be, on average, 80% shorter. We find that between 40 – 95% of Br atoms are produced from surface emissions of Br_2 and BrCl. It is possible that iodine may also play a potential role in facilitating heterogeneous bromine production through surface emissions of IBr, though observations of this compound have not yet been achieved.

The production of Br_2 is quite complex and is dependent on many factors, including the relative concentrations of bromide and chloride (among others), the availability of atmospheric oxidants, such as ozone (e.g., Oum et al., 1998; Pratt et al., 2013), the pH of the QLL or aerosol, the presence of snow phase oxidants such as H_2O_2 (Pratt et al., 2013), and the replenishment of the snowpack halides from deposited sea salts. The last of these is governed by meteorology, the proximity of open water or saline sea ice surfaces, and wind/storm events, making the accurate

Atmos. Chem. Phys. Discuss., doi:10.5194/acp-2015-1039, 2016
Manuscript under review for journal Atmos. Chem. Phys.
Published: 18 January 2016
© Author(s) 2016. CC-BY 3.0 License.

597 modeling of these processes very complex (Domine et al., 2013). Likewise, to date, it has not
598 been possible to determine the halide concentrations or pH of the QLL, and these values are
599 likely highly variable and dependent on snow and aerosol aging and deposition. In our model,
600 the Br_2 flux from the snowpack is highly sensitive to the pH, with small decreases in pH leading
601 to larger Br_2 surface fluxes. Due to the apparent importance of surface chemistry for both the
602 initiation and evolution of Arctic ozone depletion events, it is clear that more laboratory and field
603 studies are required to decipher these complex chemical and physical processes. In particular,
604 we strongly recommend studies relating to direct measurements of surface fluxes of molecular
605 halogens, as a function of conditions of temperature, snowpack composition, and pH. Further,
606 there is currently little understanding of the mechanism for Cl_2 production, and no successful
607 measurements of IO in the High Arctic. Recent observations of I_2 within the Barrow snowpack
608 (Raso et al., 2015) suggest reactive iodine chemistry is present in this region. Investigations into
609 these areas would greatly increase our understanding of halogen chemistry and ozone depletion
610 in the Arctic.
611
612 **Acknowledgements** This work was funded by the National Science Foundation grant ARC-
613 0732556. Partial support for CT during preparation of this manuscript was provided by the NSF
614 Atmospheric and Geospace Sciences Postdoctoral Research Fellowship program. The authors
615 wish to thank the organizers of the OASIS 2009 field campaign, the Barrow Arctic Science
616 Consortium for logistics support, and all of the researchers who contributed to the campaign.
617 This paper is submitted in memory of our colleague and friend, Roland von Glasow.
618
619
620

Atmos. Chem. Phys. Discuss., doi:10.5194/acp-2015-1039, 2016
Manuscript under review for journal Atmos. Chem. Phys.
Published: 18 January 2016
© Author(s) 2016. CC-BY 3.0 License.

Atmospheric Chemistry and Physics Discussions

621 **References**

622 Adams, J., Holmes, N., and Crowley, J.: Uptake and reaction of HOBr on frozen and dry
623 NaCl/NaBr surfaces between 253 and 233K, Atmos. Chem. Phys., 2, 79 – 91, doi: 10.5194/acp-
624 2-79-2002, 2002.
625
626 Barrie, L., Bottenheim, J., Schnell, R., Crutzen, P., and Rasmussen, R.: Ozone destruction and
627 photochemical reactions at polar sunrise in the lower Arctic atmosphere, Nature, 334, 138 - 141,
628 doi: 10.1038/334138a0, 1988.
629
630 Calvert, J. G., and Lindberg, S. E.: Potential influence of iodine-containing compounds on the
631 chemistry of the troposphere in the polar spring. I. Ozone depletion, Atmos. Environ., 38, 5087-
632 5104, doi: 10.1016/j.atmosenv.2004.05.049, 2004.
633
634 Carpenter, L. J., S. M. MacDonald, M. D. Shaw, R. Kumar, R.W. Saunders, R. Parthipan,
635 J.Wilson and J. M. C. Plane, Atmospheric iodine levels influenced by sea surface emissions of
636 inorganic iodine, Nature Geosci., *6,* 108-111, doi: 10.1038/ngeo1687, 2013.

637 Cavender, A., Biesenthal, T., Bottenheim, J., and Shepson, P.: Volatile organic compound ratios
638 as probes of halogen atom chemistry in the Arctic, Atmos. Chem. Phys., 8, 1737-1750, 2008.
639
640 Domine, F., J. Bock, D. Voisin, and D. J. Donaldson, Can We Model Snow Photochemistry?
641 Problems with the Current Approaches, J. Phys. Chem., A, 117, 4733−4749, doi:
642 10.1021/jp3123314, 2013.
643
644 Edwards, G. D., Cantrell, C. A., Stephens, S., Hill, B., Goyea, O., Shetter, R. E., Mauldin III, R.
645 L., Kosciuch, E., Tanner, D. J., and Eisele, F. L.: Chemical ionization mass spectrometer
646 instrument for the measurement of tropospheric HO_2 and RO_2, Anal. Chem., 75, 5317-5327, doi:
647 10.1021/ac034402b, 2003.
648
649 Ehhalt, D. H.: Photooxidation of trace gases in the troposphere Plenary Lecture, Phys. Chem.
650 Chem. Phys., 1, 5401-5408, 1999.
651
652 Fan, S-M. and D. J. Jacob, Surface ozone depletion in Arctic spring sustained by bromine
653 reactions on aerosols, Nature, 358, 522-524, 1992.
654
655 Foster, K. L., Plastridge, R. A., Bottenheim, J. W., Shepson, P. B., Finlayson-Pitts, B. J., and
656 Spicer, C. W.: The role of Br_2 and BrCl in surface ozone destruction at polar sunrise, Science,
657 291, 471-474, 2001.
658
659 Frieß, U., Deutschmann, T., Gilfedder, B., Weller, R., and Platt, U.: Iodine monoxide in the
660 Antarctic snowpack, Atmos. Chem. Phys, 10, 2439-2456, 2010.
661
662 Gladich, I., J. S. Francisco, R. J. Buszek, M. Vazdar, M. A. Caignano, and P. B. Shepson, *Ab*
663 *Initio* Study of the Reaction of Ozone with Bromide Ion, J. Phys. Chem. A, 119, 4482−4488,
664 2015.
665

© Author(s) 2016. CC-BY 3.0 License.

666 Gong, S., Walmsley, J., Barrie, L., and Hopper, J.: Mechanisms for surface ozone depletion and
667 recovery during polar sunrise, Atmos. Environ., 31, 969-981, 1997.
668
669 Guimbaud, C., Grannas, A. M., Shepson, P. B., Fuentes, J. D., Boudries, H., Bottenheim, J. W.,
670 Dominé, F., Houdier, S., Perrier, S., and Biesenthal, T. B.: Snowpack processing of acetaldehyde
671 and acetone in the Arctic atmospheric boundary layer, Atmos. Environ., 36, 2743-2752, 2002.
672
673 Hausmann, M., and Platt, U.: Spectroscopic measurement of bromine oxide and ozone in the
674 high Arctic during Polar Sunrise Experiment 1992, J. Geophys. Res., 99, 25399, 1994.
675
676 Helmig, D., Ganzeveld, L., Butler, T., and Oltmans, S.: The role of ozone atmosphere-snow gas
677 exchange on polar, boundary-layer tropospheric ozone? a review and sensitivity analysis, Atmos.
678 Chem. Phys., 7, 15-30, 2007.
679
680 Helmig, D., Boylan, P., Johnson, B., Oltmans, S., Fairall, C., Staebler, R., Weinheimer, A.,
681 Orlando, J., Knapp, D. J., Montzka, D. D., Flocke, F., Frieß, U., Sihler, H., and Shepson, P. B.:
682 Ozone dynamics and snow-atmosphere exchanges during ozone depletion events at Barrow,
683 Alaska, J. Geophys. Res., 117, D20303, doi:10.1029/2012JD017531, 2012.
684
685 Hirokawa, J., Onaka, K., Kajii, Y., and Akimoto, H.: Heterogeneous processes involving sodium
686 halide particles and ozone: molecular bromine release in the marine boundary layer in the
687 absence of nitrogen oxides, Geophys. Res. Lett., 25, 2449-2452, 1998.
688
689 Hönninger, G.: Halogen Oxide Studies in the Boundary Layer by Multi Axis Differential Optical
690 Absorption Spectroscopy and Active Longpath-DOAS, Ph.D., University of Heidelberg, 2002.
691
692 Huff, A. K., and Abbatt, J. P. D.: Kinetics and product yields in the heterogeneous reactions of
693 HOBr with ice surfaces containing NaBr and NaCl, J. Phys. Chem. A, 106, 5279-5287, 2002.
694
695 Jacob, D. J.: Heterogeneous chemistry and tropospheric ozone, Atmos. Environ., 34, 2131-2159,
696 2000.
697
698 Kuo, K. K.: Principles of combustion, John Wiley & Sons, New York, 1986.
699
700 Lary, D.: Gas phase atmospheric bromine photochemistry, J. Geophys. Res., 101, 1505-1516,
701 1996.
702
703 Le Bras, G., and Platt, U.: A possible mechanism for combined chlorine and bromine catalyzed
704 destruction of tropospheric ozone in the Arctic, Geophys. Res. Lett., 22, 599-602, 1995.
705
706 Lehrer, E., Hönninger, G., and Platt, U.: A one dimensional model study of the mechanism of
707 halogen liberation and vertical transport in the polar troposphere, Atmos. Chem. Phys., 4, 2427-
708 2440, 2004.
709

© Author(s) 2016. CC-BY 3.0 License.

710 Liao, J., Huey, L., Scheuer, E., Dibb, J., Stickel, R., Tanner, D., Neuman, J., Nowak, J., Choi, S.,
711 and Wang, Y.: Characterization of soluble bromide measurements and a case study of BrO
712 observations during ARCTAS, Atmos. Chem. Phys, 12, 1327-1338, 2012a.
713
714 Liao, J., Huey, L., Tanner, D., Flocke, F., Orlando, J., Neuman, J., Nowak, J., Weinheimer, A.,
715 Hall, S., Smith, J., Fried, A., Staebler, R., Wang, Y., Koo, J.-H., Cantrell, C., Weibring, P.,
716 Walega, J., Knapp, D., Shepson, P., and Stephens, C.: Observations of inorganic bromine (HOBr,
717 BrO, and Br_2) speciation at Barrow, Alaska, in spring 2009, J. Geophys. Res., 117, D00R16,
718 2012b.
719
720 Liao, J., L. G. Huey, Z. Liu, D. J. Tanner, C. A. Cantrell, J. J. Orlando, F. M. Flocke, P. B.
721 Shepson, A. J. Weinheimer, S. R. Hall, H. J. Beine, Y. Wang, E. D. Ingall, C. R. Stephens, R. S.
722 Hornbrook, E. Apel, A. Fried, L. Mauldin, J. N. Smith, R. M. Staebler, J.A. Neuman, J.B.
723 Nowak, High levels of molecular chlorine in the Arctic atmosphere, Nature Geosci., 7, 91 – 94,
724 doi:10.1038/ngeo2046, 2014.

725 Mahajan, A., Shaw, M., Oetjen, H., Hornsby, K., Carpenter, L., Kaleschke, L., Tian-Kunze, X.,
726 Lee, J., Moller, S., and Edwards, P.: Evidence of reactive iodine chemistry in the Arctic
727 boundary layer, J. Geophys. Res., 115, D20303, doi: 10.1029/2009JD013665, 2010.
728
729 Martinez, M., Arnold, T., and Perner, D.: The role of bromine and chlorine chemistry for arctic
730 ozone depletion events in Ny-Ålesund and comparison with model calculations, Annales
731 Geophysicae, 17, 941-956, 1999.
732
733 McFiggans, G., Plane, J. M. C., Allan, B. J., Carpenter, L. J., Coe, H., and O'Dowd, C.: A
734 modeling study of iodine chemistry in the marine boundary layer, J. Geophys. Res., 105, 14371-
735 14385, 2000.
736
737 McFiggans, G., Cox, R. A., Mössinger, J. C., Allan, B. J., and Plane, J. M. C.: Active chlorine
738 release from marine aerosols: Roles for reactive iodine and nitrogen species, J. Geophys. Res,
739 107, doi: 10.1029/2001JD000383, 2002.
740
741 Michalowski, B. A., Francisco, J. S., Li, S. M., Barrie, L. A., Bottenheim, J. W., and Shepson, P.
742 B.: A computer model study of multiphase chemistry in the Arctic boundary layer during polar
743 sunrise, J. Geophys. Res., 105, 15131 – 15145, 2000.
744
745 Monks, P. S.: Gas-phase radical chemistry in the troposphere, Chem. Soc. Rev., 34, 376-395,
746 2005.
747
748 Oum, K., Lakin, M., DeHaan, D., Brauers, T., and Finlayson-Pitts, B.: Formation of molecular
749 chlorine from the photolysis of ozone and aqueous sea-salt particles, Science, 279, 74, 1998a.
750
751 Oum, K., Lakin, M., and Finlayson-Pitts, B.: Bromine activation in the troposphere by the dark
752 reaction of O_3 with seawater ice, Geophys. Res. Lett., 25, 3923-3926, 1998b.
753
754 Piot, M., and Von Glasow, R.: The potential importance of frost flowers, recycling on snow, and
755 open leads for ozone depletion events, Atmos. Chem. Phys., 8, 2437-2467, 2008.

© Author(s) 2016. CC-BY 3.0 License.

Platt, U., and Janssen, C.: Observation and role of the free radicals NO_3, ClO, BrO and IO in the troposphere, Faraday Discuss., 100, 175-198, 1995.

Pöhler, D., Vogel, L., Frieß, U., and Platt, U.: Observation of halogen species in the Amundsen Gulf, Arctic, by active long-path differential optical absorption spectroscopy, Proceedings of the National Academy of Sciences, 107, 6582, 2010.

Pratt, K. A., Custard, K. D., Shepson, P. B., Douglas, T. A., Pöhler, D., General, S., Zielcke, J., Simpson, W. R., Platt, U., Tanner, D. J., Huey, L. G., Carlsen, M., and Stirm, B. H.: Photochemical production of molecular bromine in Arctic surface snowpacks, Nature Geosci., 6, 351 – 356, doi: 10.1038/ngeo1779, 2013.

Raso, A. R. W., Custard, K. D., Pratt, K. A., Tanner, D. J., Huey, L. G., and Shepson, P. B.: Active molecular iodine snowpack photochemistry in the Arctic, J. Geophys. Res., submitted, 2015.

Saiz-Lopez, A., Mahajan, A. S., Salmon, R. A., Bauguitte, S. J. B., Jones, A. E., Roscoe, H. K., and Plane, J. M. C.: Boundary layer halogens in coastal Antarctica, Science, 317, 348-351, 2007.

Saiz-Lopez, A., Plane, J. M. C., Mahajan, A. S., Anderson, P. S., Bauguitte, S. J. B., Jones, A. E., Roscoe, H. K., Salmon, R. A., Bloss, W. J., and Lee, J. D.: On the vertical distribution of boundary layer halogens over coastal Antarctica: implications for O_3, HO_x, NO_x and the Hg lifetime, Atmos. Chem. Phys., 8, 887-900, 2008.

Shetter, R. E., and Müller, M.: Photolysis frequency measurements using actinic flux spectroradiometry during the PEM-Tropics mission: Instrumentation description and some results, J. Geophys. Res., 104, 5647-5661, 1999.

Shepson, P. B., Sirju, A.-P., Hopper, J. F., Barrie, L. A., Young, V., Niki, H. and Dryfhout, H.: Sources and sinks of carbonyl compounds in the Arctic Ocean boundary layer: a polar icefloe experiment, J. Geophys. Res., 101, 21081 - 21089, 1996.

Stephens, C. R., Shepson, P. B., Steffen, A., Bottenheim, J. W., Liao, J., Huey, L. G., Apel, E., Weinheimer, A., Hall, S. R., and Cantrell, C.: The relative importance of chlorine and bromine radicals in the oxidation of atmospheric mercury at Barrow, Alaska, J. Geophys. Res., 117, D00R11, doi: 10.1029/2011JD016649, 2012.

Sturges, W., and Barrie, L.: Chlorine, bromine and iodine in Arctic aerosols, Atmos. Environ., 22, 1179-1194, 1988.

Tang, T., and McConnell, J.: Autocatalytic release of bromine from Arctic snow pack during polar sunrise, Geophys. Res. Lett., 23, 2633-2636, 1996.

Thompson, C. R., Shepson, P. B., Liao, J., Huey, L. G., Apel, E. C., Cantrell, C. A., Flocke, F., Orlando, J., Fried, A., Hall, S. R., Hornbrook, R. S., Knapp, D. J., Mauldin III, R. L., Montzka,

Atmos. Chem. Phys. Discuss., doi:10.5194/acp-2015-1039, 2016
Manuscript under review for journal Atmos. Chem. Phys.
Published: 18 January 2016
© Author(s) 2016. CC-BY 3.0 License.

Atmospheric Chemistry and Physics Discussions

D. D., Sive, B. C., Ullmann, K., Weibring, P. and Weinheimer, A.: Interactions of bromine, chlorine, and iodine photochemistry during ozone depletions in Barrow, Alaska, Atmos. Chem. Phys., 15, 9651 – 9679, doi: 10.5194/acp-15-9651-2015, 2015.

Vogt, R., Crutzen, P. J., and Sander, R.: A mechanism for halogen release from sea-salt aerosol in the remote marine boundary layer, Nature, 383, 327 – 330, doi: 10.1038/383327a0, 1996.

Vogt, R., Sander, R., von Glasow, R., and Crutzen, P. J.: Iodine chemistry and its role in halogen activation and ozone loss in the marine boundary layer: A model study, J. Atmos. Chem., 32, 375-395, 1999.

Wennberg, P., Hanisco, T., Jaegle, L., Jacob, D., Hintsa, E., Lanzendorf, E., Anderson, J., Gao, R. S., Keim, E., and Donnelly, S.: Hydrogen radicals, nitrogen radicals, and the production of O_3 in the upper troposphere, Science, 279, 49-53, 1998.

Zeng, T., Wang, Y., Chance, K., Blake, N., Blake, D., and Ridley, B.: Halogen-driven low-altitude O_3 and hydrocarbon losses in spring at northern high latitudes, J. Geophys. Res, 111, D17, doi: 10.1029/2005JD006706, 2006.

Table 1. Reactions used in the model that are pertinent to bromine chemistry. All rate constants (with the exception of photolysis *J* coefficients) are in units of cm^3 $molecule^{-1}$ s^{-1}.

Gas-Phase Reactions	**Rate Constant**	**Reference**
$Br + O_3 \rightarrow BrO$	6.75×10^{-13}	*Atkinson et al.* [2004]
$Br + C_2H_4 \rightarrow HBr + C_2H_5OO$	1.3×10^{-13}	*Atkinson et al.* [2004]
$Br + C_3H_6 \rightarrow HBr + C_3H_5$	1.60×10^{-12}	*Atkinson et al.* [2004]
$Br + HCHO \rightarrow HBr + CO + HO_2$	6.75×10^{-13}	*Sander et al.* [2006]
$Br + CH_3CHO \rightarrow HBr + CH_3COOO$	2.8×10^{-12}	*Atkinson et al.* [2004]
$Br + C_3H_6O \rightarrow HBr$	9.7×10^{-12}	*Wallington et al.* [1989]
Br + nButanal → HBr	9.7×10^{-12}	estimate from *Michalowski et al.* [2000]
$Br + CH_3OOH \rightarrow HBr + CH_3OO$	4.03×10^{-15}	*Mallard et al.* [1993]
$Br + NO_2 \rightarrow BrNO_2$	2.7×10^{-11}	*Atkinson et al.* [2004]
$Br + BrNO_3 \rightarrow Br_2 + NO_3$	4.9×10^{-11}	*Orlando and Tyndall* [1996]
$Br + OClO \rightarrow BrO + ClO$	1.43×10^{-13}	*Atkinson et al.* [2004]
$BrO + O(^3P) \rightarrow Br$	4.8×10^{-11}	*Atkinson et al.* [2004]
$BrO + OH \rightarrow Br + HO_2$	4.93×10^{-11}	*Atkinson et al.* [2004]
$BrO + HO_2 \rightarrow HOBr$	3.38×10^{-11}	*Atkinson et al.* [2004]
$BrO + CH_3OO \rightarrow HOBr + CH_2OO$	4.1×10^{-12}	*Aranda et al.* [1997]
$BrO + CH_3OO \rightarrow Br + HCHO + HO_2$	1.6×10^{-12}	*Aranda et al.* [1997]
$BrO + CH_3COOO \rightarrow Br + CH_3COO$	1.7×10^{-12}	estimate from *Michalowski et al.* [2000]
$BrO + C_3H_6O \rightarrow HOBr$	1.5×10^{-14}	estimate from *Michalowski et al.* [2000]
$BrO + NO \rightarrow Br + NO_2$	2.48×10^{-11}	*Atkinson et al.* [2004]
$BrO + NO_2 \rightarrow BrNO_3$	1.53×10^{-11}	*Atkinson et al.* [2004]
$BrO + BrO \rightarrow Br + Br$	2.82×10^{-12}	*Sander et al.* [2006]
$BrO + BrO \rightarrow Br_2$	9.3×10^{-13}	*Sander et al.* [2006]
$BrO + HBr \rightarrow HOBr + Br$	2.1×10^{-14}	*Hansen et al.* [1999]
$HBr + OH \rightarrow Br + H_2O$	1.26×10^{-11}	*Sander et al.* [2006]
$CH_3Br + OH \rightarrow H_2O + Br$	1.27×10^{-14}	*Atkinson et al.* [2004]
$CHBr_3 + OH \rightarrow H_2O + Br$	1.2×10^{-13}	*Atkinson et al.* [2004]
$Cl + BrCl \leftrightarrow Br + Cl_2$	f: 1.5×10^{-11} r: 1.1×10^{-15}	*Clyne et al.* [1972]

Atmos. Chem. Phys. Discuss., doi:10.5194/acp-2015-1039, 2016
Manuscript under review for journal Atmos. Chem. Phys.
Published: 18 January 2016
© Author(s) 2016. CC-BY 3.0 License.

Atmospheric Chemistry and Physics Discussions

$Cl + Br_2 \leftrightarrow BrCl + Br$	f: 1.2×10^{-10} r: 3.3×10^{-15}			*Clyne et al.* [1972]
$BrO + ClO \rightarrow Br + Cl$	7.04×10^{-12}			*Atkinson et al.* [2004]
$BrO + ClO \rightarrow BrCl$	1.15×10^{-12}			*Atkinson et al.* [2004]
$BrO + ClO \rightarrow Br + OClO$	9.06×10^{-12}			*Atkinson et al.* [2004]
$HOBr + OH \rightarrow BrO + H_2O$	5.0×10^{-13}			*Kukui et al.* [1996]
$HOBr + Cl \rightarrow BrCl + OH$	8.0×10^{-11}			*Kukui et al.* [1996]
$HOBr + O(^3P) \rightarrow BrO + OH$	2.12×10^{-11}			*Atkinson et al.* [2004]
$IO + BrO \rightarrow Br + OIO$	9.36×10^{-11}			*Atkinson et al.* [2004]
$IO + BrO \rightarrow IBr$	4.32×10^{-11}			*Atkinson et al.* [2004]
$IO + BrO \rightarrow Br + I$	7.2×10^{-12}			*Atkinson et al.* [2004]
Photolysis Reactions	**J_{max} (25 March) s^{-1}**	**Lifetime**	**Reference**	
$BrNO_3 \rightarrow Br + NO_3$	2.1×10^{-4}	1.3 h	calculated from OASIS data	
$BrNO_3 \rightarrow BrO + NO_2$	1.2×10^{-3}	14.2 min	calculated from OASIS data	
$BrO \rightarrow Br + O(^3P)$	3.0×10^{-2}	33 s	calculated from OASIS data	
$Br_2 \rightarrow Br + Br$	4.4×10^{-2}	23 s	calculated from OASIS data	
$HOBr \rightarrow Br + OH$	2.3×10^{-3}	7.2 min	calculated from OASIS data	
$BrNO_2 \rightarrow Br + NO_2$	1.5×10^{-4}	1.8 h	estimate from *Lehrer et al.* [2004]	
$BrCl \rightarrow Br + Cl$	1.26×10^{-2}	1.3 min	calculated from OASIS data	
Mass Transfer Reactions	**k_t (forward)**	**k_t (reverse)**		
$HBr_{(g)} \rightarrow H^+_{(p)} + Br^-_{(p)}$	1.80×10^{-3}			
$HOBr_{(g)} \rightarrow HOBr_{(p)}$	1.26×10^{-3}			
$Br_{2(g)} \leftrightarrow Br_{2(p)}$	1.78×10^{-5}	2.97×10^{8}		
$BrCl_{(g)} \leftrightarrow BrCl_{(p)}$	6.60×10^{-4}	1.91×10^{10}		
$IBr_{(p)} \rightarrow IBr_{(g)}$	5.53×10^{9}			
$HBr_{(g)} \rightarrow H^+_{(s)} + Br^-_{(s)}$	1.67×10^{-5}			
$HOBr_{(g)} \rightarrow HOBr_{(s)}$	1.67×10^{-5}			
$Br_{2(g)} \leftrightarrow Br_{2(s)}$	1.0×10^{-5}	7.71×10^{-2}		
$BrCl_{(g)} \leftrightarrow BrCl_{(s)}$	1.25×10^{-5}	7.71×10^{-2}		
$IBr_{(s)} \rightarrow IBr_{(g)}$	7.71×10^{-2}			
Aqueous Phase Reactions	**k (particle)**	**k (snow)**	**Reference**	
$Cl^- + HOBr + H^+ \rightarrow BrCl$	5.17×10^{21}	9.30×10^{26}	*Wang et al.* [1994]	
$Br^- + HOCl + H^+ \rightarrow BrCl$	1.2×10^{24}	2.15×10^{29}	*Sander et al.* [1997]	
$Br^- + HOBr + H^+ \rightarrow Br_2$	1.47×10^{20}	2.64×10^{25}	*Beckwith et al.* [1996]	
$Br^- + HOI + H^+ \rightarrow IBr$	3.04×10^{18}	5.46×10^{23}	*Troy et al.* [1991]	
$BrCl + Cl^- \rightarrow BrCl_2^-$	3.3	5.99×10^{5}	*Michalowski et al.* [2000]	
$BrCl_2^- \rightarrow BrCl + Cl^-$	1.58×10^{9}	1.58×10^{9}	*Michalowski et al.* [2000]	
$BrCl + Br^- \rightarrow Br_2Cl^-$	3.3	5.99×10^{5}	*Michalowski et al.* [2000]	
$Br_2Cl^- \rightarrow BrCl + Br^-$	3.34×10^{5}	3.34×10^{5}	*Wang et al.* [1994]	
$Cl_2 + Br^- \rightarrow BrCl_2^-$	4.27	7.66×10^{5}	*Wang et al.* [1994]	
$BrCl_2^- \rightarrow Cl_2 + Br^-$	6.94×10^{2}	6.94×10^{2}	*Wang et al.* [1994]	
$O_3 + Br^- \rightarrow HOBr$	4.5×10^{-9}	8.08×10^{-14}	*Oum et al.* [1998]	

Table 2. Median mid-day bromine chain lengths for 25, 29, and 30 March 2009 (days with O_3 present) determined for four different modeling scenarios with different combinations of halogens present. Method 1 refers to Equation 3 (using terminations reactions) and Method 2 refers to Equation 4 (using initiation reactions).

Atmos. Chem. Phys. Discuss., doi:10.5194/acp-2015-1039, 2016
Manuscript under review for journal Atmos. Chem. Phys.
Published: 18 January 2016
© Author(s) 2016. CC-BY 3.0 License.

Atmospheric Chemistry and Physics Discussions

	25 March		29 March		30 March		Average (1-σ st. deviation)	
	Method 1	Method 2	Method 1	Method 2	Method 1	Method 2	Method 1	Method 2
Br only	1.27	1.36	1.50	1.03	1.78	1.11	1.51 (± 0.25)	1.17 (± 0.17)
Br and Cl	1.26	1.34	1.41	0.97	1.55	1.09	1.41 (± 0.15)	1.13 (± 0.19)
Br and Low I	1.44	1.36	1.61	1.10	1.96	1.18	1.67 (± 0.27)	1.21 (± 0.13)
Br and High I	1.36	1.36	1.58	1.06	1.80	1.14	1.58 (± 0.22)	1.19 (± 0.15)
Br, Cl, and Low I	1.35	1.34	1.51	1.00	1.62	1.11	1.49 (± 0.14)	1.15 (± 0.17)
Br, Cl, and High I	1.42	1.34	1.60	1.04	1.73	1.13	1.58 (± 0.16)	1.17 (± 0.15)

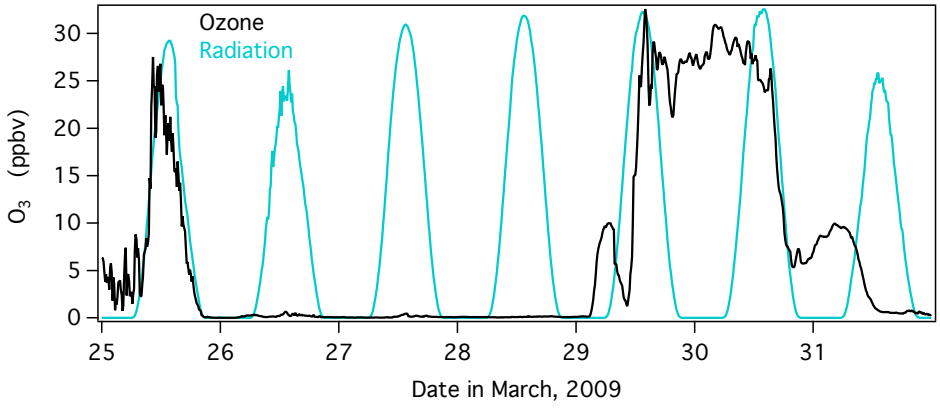

Fig 1. Time series of ambient ozone mixing ratios during OASIS for the seven-day period simulated from 25 March through 31 March 2009. Time expressed in Alaska Standard Time. Radiation is shown as the cyan trace as a reference.

Atmos. Chem. Phys. Discuss., doi:10.5194/acp-2015-1039, 2016
Manuscript under review for journal Atmos. Chem. Phys.
Published: 18 January 2016
© Author(s) 2016. CC-BY 3.0 License.

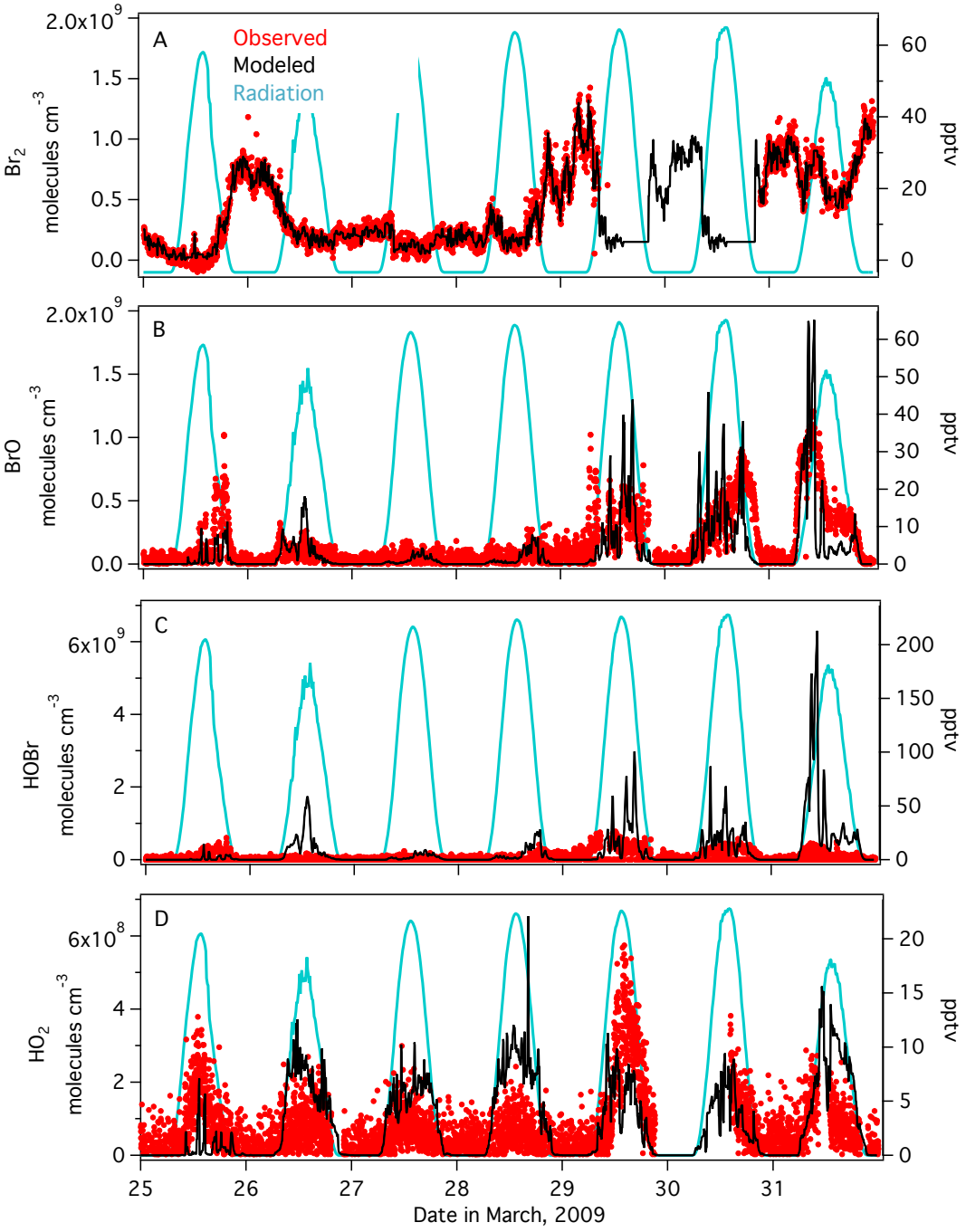

Fig 2. Comparisons of modeled (black trace) versus measured (red data) gas-phase concentrations of BrO, Br_2, and HO_2 for the seven-day period simulated. Radiation is shown as the cyan trace as a reference. Time is expressed in Alaska Standard Time.

Atmos. Chem. Phys. Discuss., doi:10.5194/acp-2015-1039, 2016
Manuscript under review for journal Atmos. Chem. Phys.
Published: 18 January 2016
© Author(s) 2016. CC-BY 3.0 License.

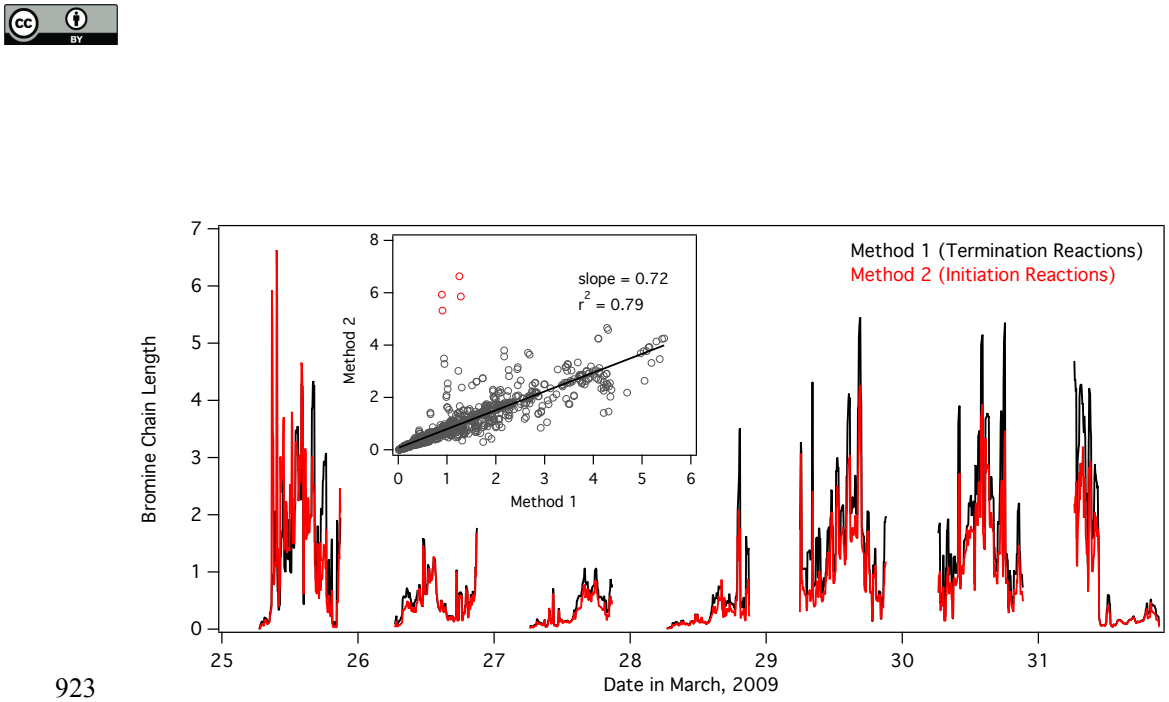

Fig 3. Daytime only bromine chain length 7-day time-series calculated from the multiday model. Method 1 is plotted as the black trace and Method 2 is plotted as the red trace. The inset graph shows a linear regression of Method 1 and Method 2 calculations. Time is expressed in Alaska Standard Time.

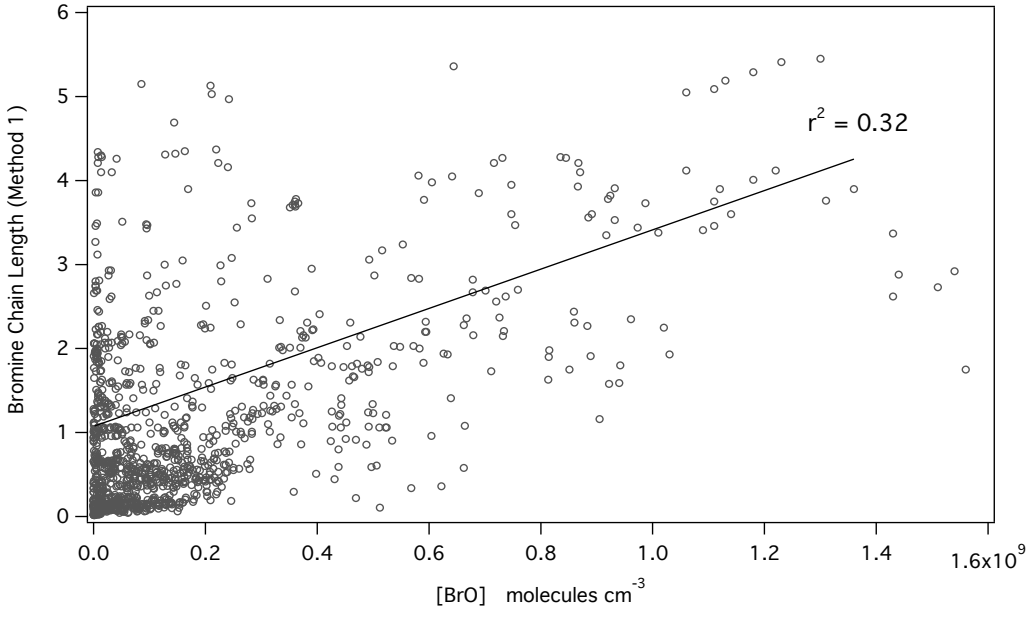

Fig 4. Regression of daytime bromine chain length calculated by Method 1 (Equation 5) and simulated BrO concentration.

Atmos. Chem. Phys. Discuss., doi:10.5194/acp-2015-1039, 2016
Manuscript under review for journal Atmos. Chem. Phys.
Published: 18 January 2016
© Author(s) 2016. CC-BY 3.0 License.

Atmospheric Chemistry and Physics Discussions

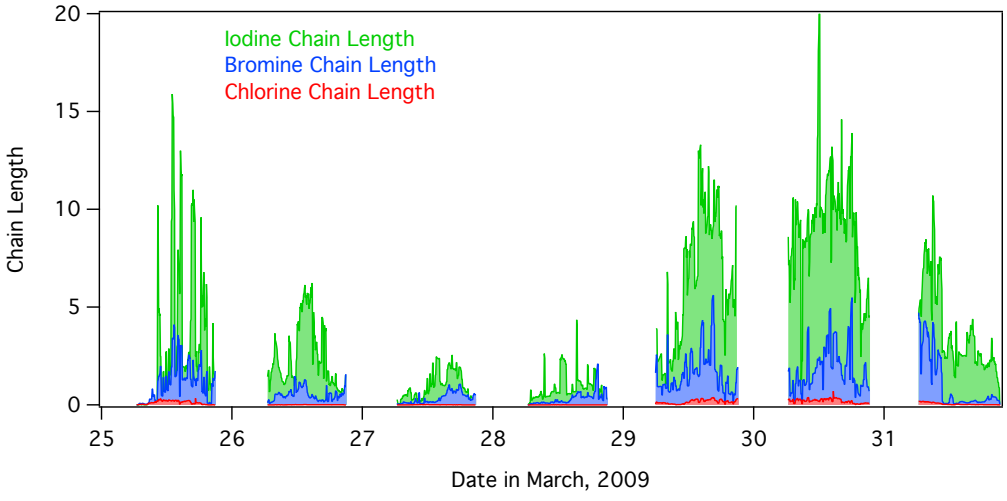

932

933 **Fig 5.** Calculated chain lengths for iodine (green), bromine (blue), and chlorine (red) across the
934 seven days of the simulated period modeled using the Base + Low Iodine scenario.

935

936

Atmos. Chem. Phys. Discuss., doi:10.5194/acp-2015-1039, 2016
Manuscript under review for journal Atmos. Chem. Phys.
Published: 18 January 2016
© Author(s) 2016. CC-BY 3.0 License.

Atmospheric Chemistry and Physics Discussions

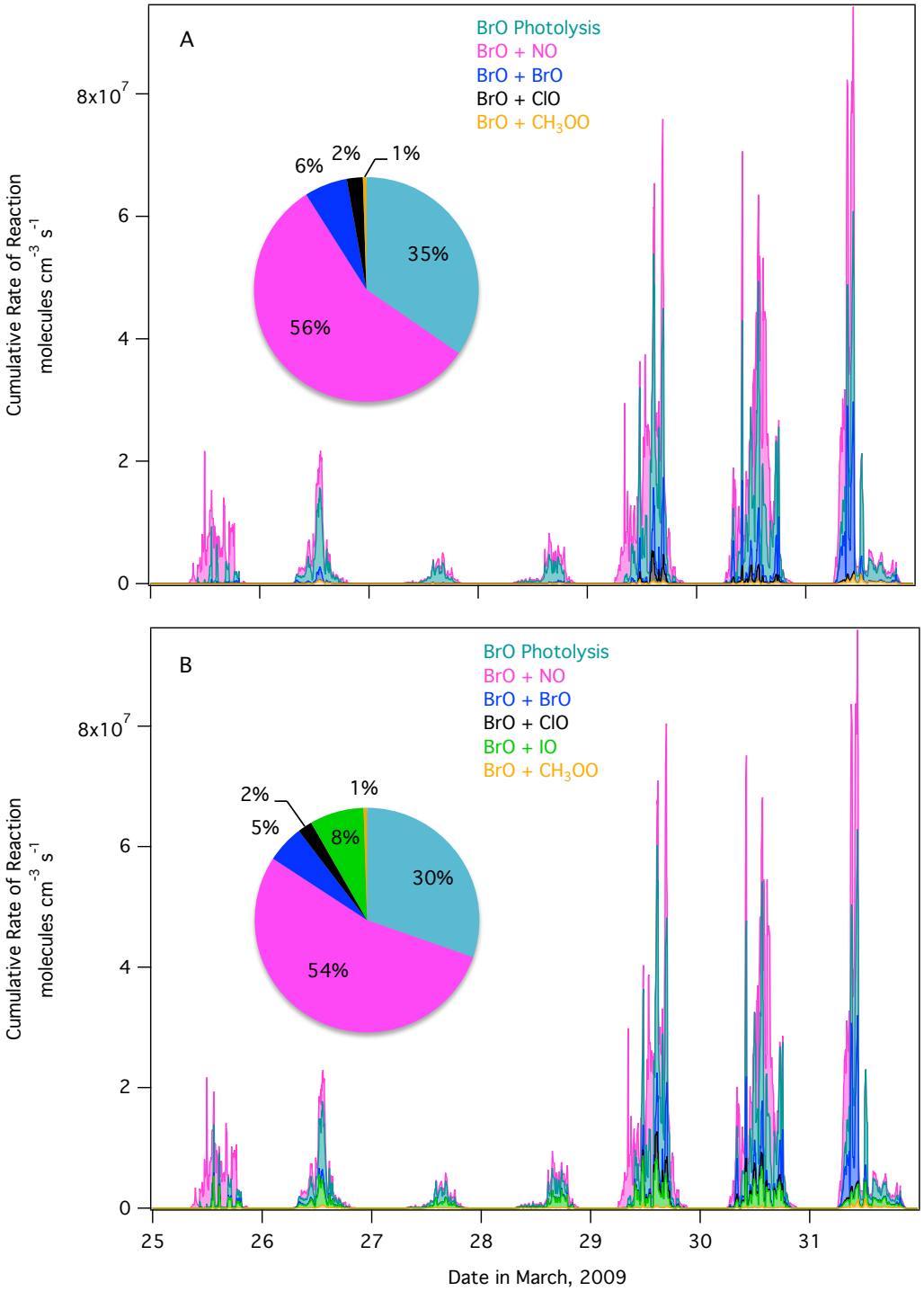

Atmos. Chem. Phys. Discuss., doi:10.5194/acp-2015-1039, 2016
Manuscript under review for journal Atmos. Chem. Phys.
Published: 18 January 2016
© Author(s) 2016. CC-BY 3.0 License.

Atmospheric Chemistry and Physics Discussions

Fig 6. Time-varying rates of the most important bromine propagation reactions in the Base Model with Br and Cl present (Panel A) and with High Iodine included (Panel B). The BrO + BrO reaction is calculated as $2k[BrO]^2$ as this reaction regenerates two Br atoms. The y-axis is expressed as a cumulative rate of reaction. Time is expressed in Alaska Standard Time. The inset pie charts shows the average fractional importance of each reaction pathway for only days 29 and 30 March (i.e. background O_3 days).

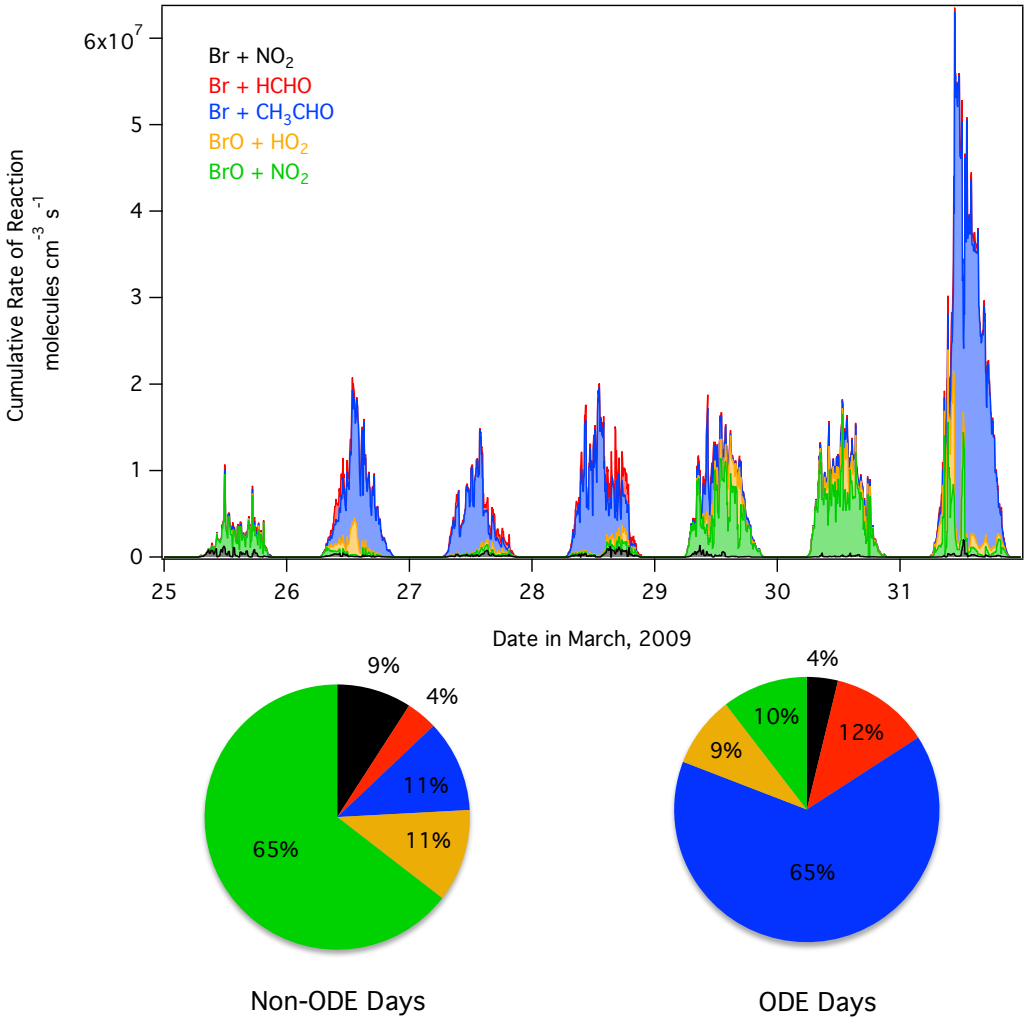

Fig 7. Time-varying rates of the most important reactive bromine (BrO_x) termination reactions in the Base Model with Br and Cl present. The y-axis is expressed as a cumulative rate of reaction. Time is expressed in Alaska Standard Time. The pie charts show the average fractional importance of each reactive bromine sink divided by non-ODE (background O_3) days and ODE days.

Atmos. Chem. Phys. Discuss., doi:10.5194/acp-2015-1039, 2016
Manuscript under review for journal Atmos. Chem. Phys.
Published: 18 January 2016
© Author(s) 2016. CC-BY 3.0 License.

Atmospheric Chemistry and Physics Discussions

951

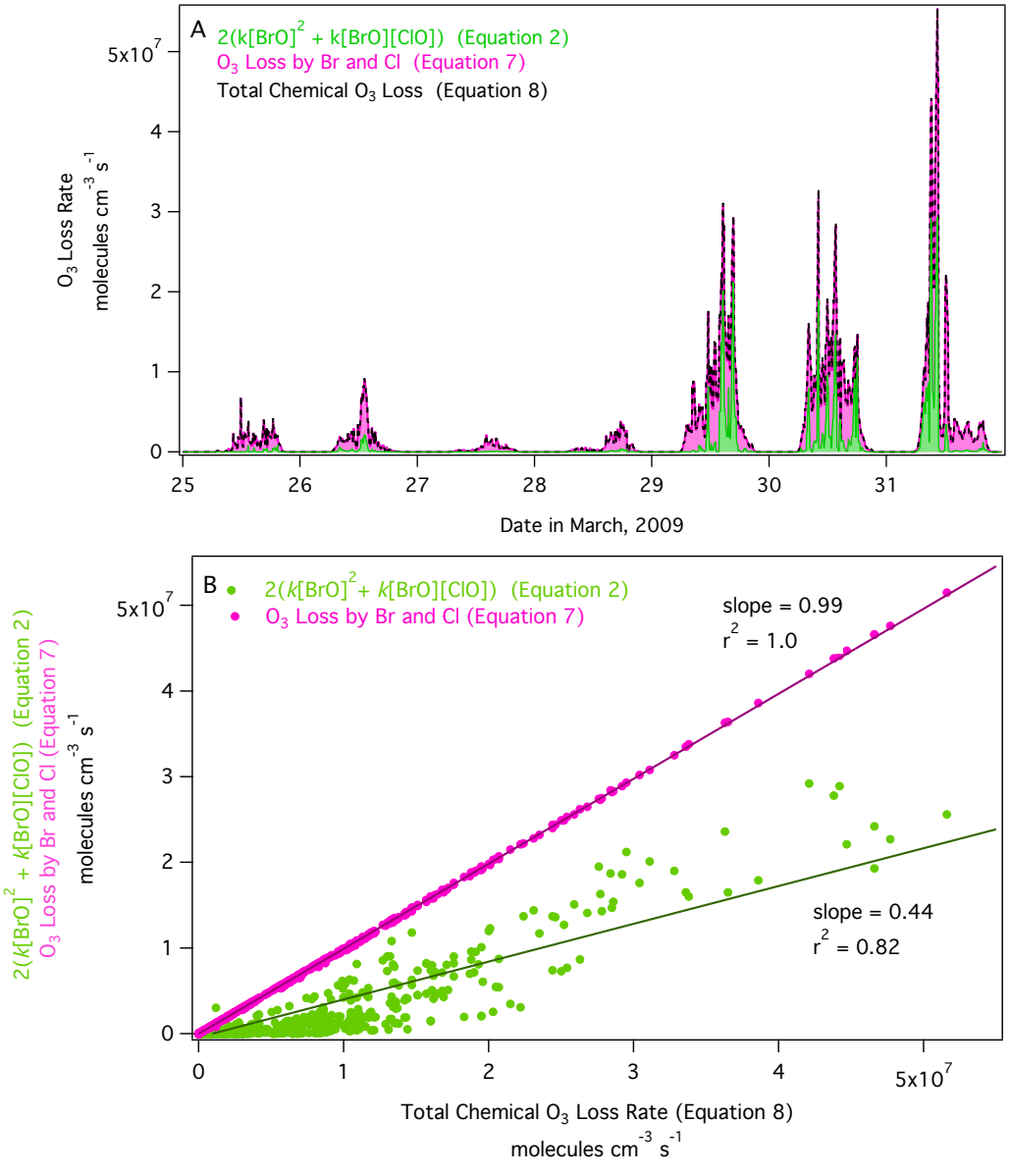

952

953 **Fig 8.** A) Comparison of the time-varying O_3 loss rate calculated using the estimation of
954 $2(k[BrO]^2 + k[BrO][ClO])$ (Equation 2, green trace), the simulated O_3 loss rate by Br and Cl
955 (Equation 7, pink trace), and the total simulated chemical O_3 loss rate (Equation 8, dashed black
956 trace). Time is expressed in Alaska Standard Time. B) Shown is a regression of $2(k[BrO]^2 +$
957 $[BrO][ClO])$ (Equation 2) versus the total simulated chemical O_3 loss rate in the Base Model
958 (Equation 8) in the green data, and a regression of O_3 loss rate by Br and Cl only (Equation 7)

Atmos. Chem. Phys. Discuss., doi:10.5194/acp-2015-1039, 2016
Manuscript under review for journal Atmos. Chem. Phys.
Published: 18 January 2016
© Author(s) 2016. CC-BY 3.0 License.

Atmospheric Chemistry and Physics Discussions

959 versus the total simulated chemical O_3 loss rate in the pink data. The slopes represent the
960 fraction of the chemical O_3 loss rate that can be accounted for by each method. For the
961 conditions simulated, the commonly used estimation method of $2(k[BrO]^2 + [BrO][ClO])$ only
962 accounts for 44% of the chemical O_3 loss rate.

963

Atmos. Chem. Phys. Discuss., doi:10.5194/acp-2015-1039, 2016
Manuscript under review for journal Atmos. Chem. Phys.
Published: 18 January 2016
© Author(s) 2016. CC-BY 3.0 License.

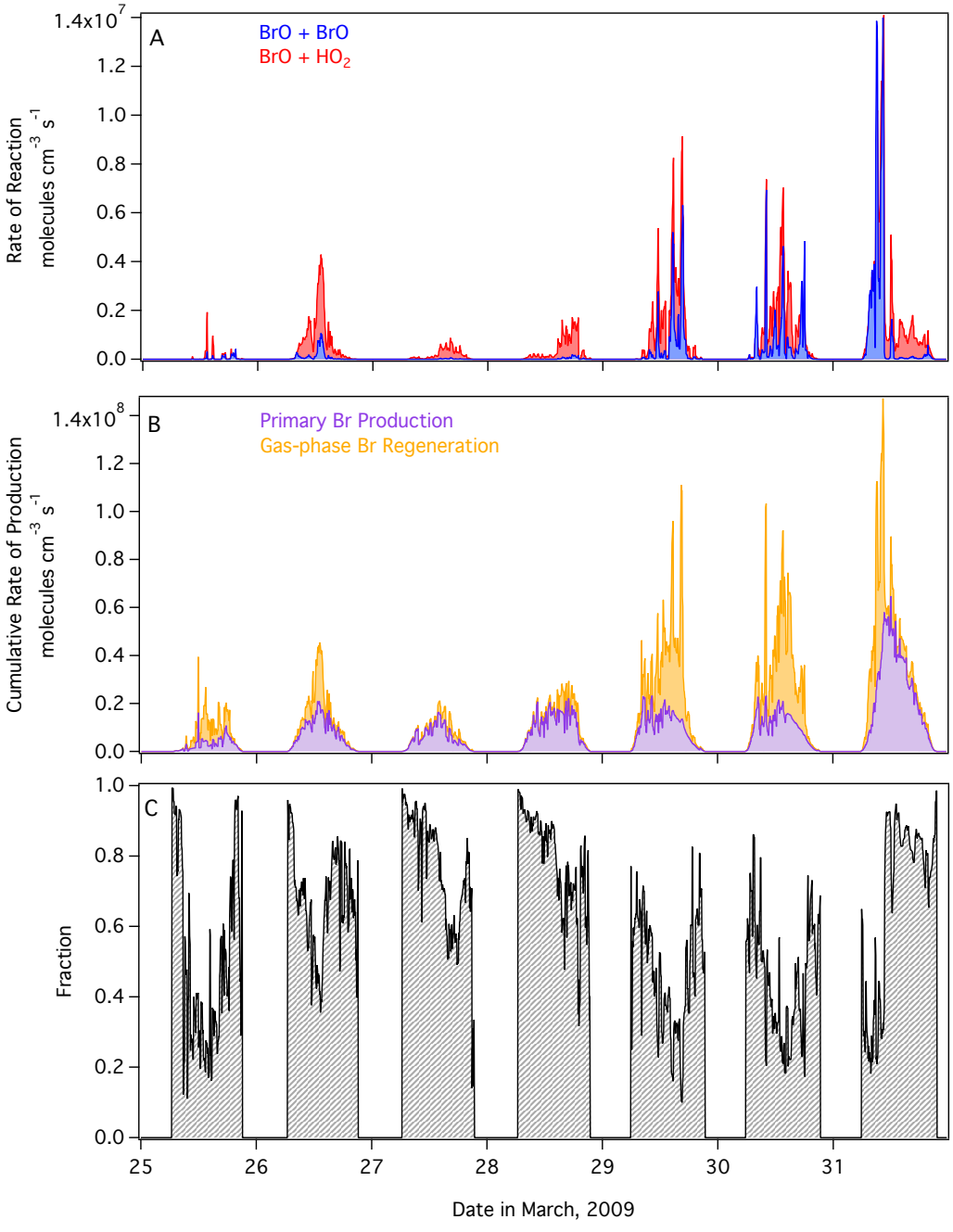

964

965 **Fig 9.** Panel A: Comparison of the reaction rates of BrO + BrO (blue) and BrO + HO_2 (red).
966 Panel B: The cumulative rate of Br atom production divided to show the primary Br production
967 rate from the photolysis of Br_2 and BrCl surface emissions calculated from Equation 9 (purple)
968 and the Br atom production rate due to gas-phase radical recycling calculated from Equation 10

Atmos. Chem. Phys. Discuss., doi:10.5194/acp-2015-1039, 2016
Manuscript under review for journal Atmos. Chem. Phys.
Published: 18 January 2016
© Author(s) 2016. CC-BY 3.0 License.

Atmospheric Chemistry and Physics Discussions

(orange). Panel C: The fraction of total Br atom production due to primary production from Br_2 and BrCl surface emissions.